Pergamon

PII: S0277-5387(96)00610-9

Polyhedron Vol. 16, No. 18, pp. 3139–3163, 1997

0277-5387/97 $17.00+0.00

Homogeneous models for hydrodenitrogenation catalysis

Keith J. Weller,* Peter A. Fox,† Steven D. Gray‡ and David E. Wigley§

Department of Chemistry, University of Arizona, Tucson, AZ 85721, U.S.A.

Abstract—Hydrodenitrogenation (HDN) catalysis is the process of removing nitrogen from petroleum feedstocks in the form of NH_3 to provide more processable and environmentally compatible liquid fuels. In practice, HDN is carried out simultaneously with other catalytic hydrotreating reactions such as hydrodesulfurization (HDS), yet HDN is significantly less well-studied than HDS. This contribution provides an overview of the heterogeneous HDN process, then outlines various homogeneous models for hydrodenitrogenation catalysis including binding modes of HDN substrates, catalytic hydrogenation processes and recent C—N bond cleavage reactions of nitrogen heterocycles. Emphasis is placed on aryloxide and alkoxide complexes of the early metals that afford some of the best homogeneous models for hydrodenitrogenation catalysis to date. © 1997 Elsevier Science Ltd

Keywords: hydrodenitrogenation; hydrotreating; catalysis; petroleum; tantalum.

INTRODUCTION

Hydrodenitrogenation (HDN) catalysis is the process of removing nitrogen from petroleum feedstocks and coal-derived liquids (in the form of NH_3) to provide more processable and environmentally sound liquid fuels. Performing HDN is essential to reduce the emissions of NO_x upon burning these fuels and because nitrogen-containing compounds seriously reduce the activity of hydrocracking and reforming catalysts used to upgrade these feedstocks. However, despite the commercial importance of this process in producing high-quality, low-cost fuels, the intimate mechanisms of simple, metal-catalysed HDN reactions are not well understood. Most HDN studies have been performed with supported, heterogeneous catalysts which have provided a wealth of data concerning product distributions, kinetics and selectivity. Our current understanding of HDN originates primarily from these studies since data from soluble, homogeneous systems are comparatively scarce. Recently, however, soluble HDN model systems under development have uncovered rather detailed structural and reactivity information that appears extremely relevant to improving our understanding of HDN. It is the intent of this contribution to provide an overview of these models with an emphasis on our studies using aryloxide supported complexes of the early transition metals. Background data from both soluble and supported catalyst systems are presented, including binding modes of HDN substrates, heterocycle hydrogenation studies, C—N bond scission mechanisms in nitrogen heterocycles and methods by which further degradation of HDN substrates may occur after C—N bond cleavage. There are several excellent overviews of HDN catalysis that focus primarily on heterogeneous systems that the reader may find useful [1–6].

OVERVIEW OF HYDRODENITROGENATION CATALYSIS

This section will briefly review HDN catalysis and outline specific problems in our current understanding of this process. We will focus on the heterogeneous practice of HDN by examining nitrogen-containing compounds subject to HDN, potential modes by which they interact with the active site and general HDN reaction schemes. We will also examine current C—N bond scission proposals in light of recent mechanistic results that may allow a more clear elucidation of the metal's role in this reaction.

* Present address: Witco Corporation, OrganoSilicones Group, Tarrytown, New York, U.S.A.

† Present address: Chiang Mai University, Chiang Mai, Thailand.

‡ Present address: Fina Oil and Chemical Company, Deer Park, Texas, U.S.A.

§ Author to whom correspondence should be addressed.

1. *Nitrogen-containing compounds subject to HDN catalysis*

Both heterocyclic nitrogen-containing compounds (principally those containing six-membered pyridine and five-membered pyrrole rings) and nonheterocyclic nitrogen compounds (aliphatic amines and anilines) are found as contaminants in petroleum and are subject to HDN catalysis [7]. However, under normal "hydrotreating" conditions, amines and anilines undergo HDN quite rapidly, therefore, industry is most concerned with the heterocyclic compounds that are among the most demanding substrates to process. The complexity of crude oil and the difficulty in studying its HDN catalysis has led to the examination of model compounds that resemble the nitrogen contaminants in petroleum, such as those shown in Fig. 1 [3,7–9]. Among these heterocycles, it is likely that the five- and six-membered rings will interact with the acidic catalyst/support differently: the six-membered pyridines are very basic at nitrogen and therefore easy to protonate or interact with acidic sites through nitrogen, while the five-membered pyrroles are more difficult to protonate but more likely to interact through their π-electron system [10]. We will primarily describe representative model complexes of the basic component, *viz.* pyridine and quinoline, and our inquiry will extend to the saturated and partially saturated forms of these substrates.

2. *Active site structure and function*

In practice, hydrodenitrogenation is carried out simultaneously with other hydrotreating reactions [e.g. hydrodesulfurization (HDS), hydrodeoxygenation (HDO) and hydrodemetallation (HDM)] and is accompanied by hydrocracking reactions and the hydrogenation of aromatics [hydrodearomatization (HDA)] [10]. However, hydrotreating parameters are usually *optimized* for only one of these processes, most often HDS. Industrial HDN is generally effected over sulfided $CoMo/\gamma\text{-}Al_2O_3$ or $NiMo/\gamma\text{-}Al_2O_3$ under rather severe hydrogenation conditions (e.g. 350–500°C and 200 atm H_2) that ultimately removes the nitrogen as NH_3 [5,10,11]. These catalysts are typically prepared by impregnating $\gamma\text{-}Al_2O_3$ with aqueous solutions of $[NH_4]_6[Mo_7O_{24}]$, along with a nickel or cobalt promotor such as $Co(NO_3)_3$ [11]. The impregnated alumina is then calcined (heated in air to afford oxide phases) and then sulfided (with H_2S, thiophene or simply a sulfur-rich feed) to generate the active hydrotreating catalyst.

The most active site for HDN reactions in this sulfided CoMo catalyst appears to be crystallites of MoS_2 (supported on γ-alumina), with Co atoms adsorbed along the edges of the MoS_2 layered structure [11]. A Mo—S site of this "CoMoS" phase is usually associated with nitrogen heterocycle activation while hydrogen is often described as dissociatively bound to sulfur in the form of sulfhydryl groups [5,10,11]. Evidence has been presented to suggest an electron transfer role for cobalt in HDN reactions [12], while others have suggested a role in hydrogen transfer [5]. Finally, several non-molybdenum catalysts have also been used in HDN such as vanadium [5], niobium sulfides [13], ruthenium sulfide [14,15], both NiW/Al_2O_3 and NiW/zeolite phases [5], molybdenum nitrides [16], as well as nonalumina supports [17,18]. We note that numerous metals other than molybdenum have been shown to catalyse HDS reactions (and presumably HDN) and often generate more active sulfide phases under catalytic hydrotreating conditions. For example, Ru, Os, Rh and Ir generate some of the most active catalytic sites for dibenzothiophene HDS [19,20].

3. *Possible substrate binding modes*

Structural aspects of binding nitrogen heterocycles to the active site of an HDN catalyst are of con-

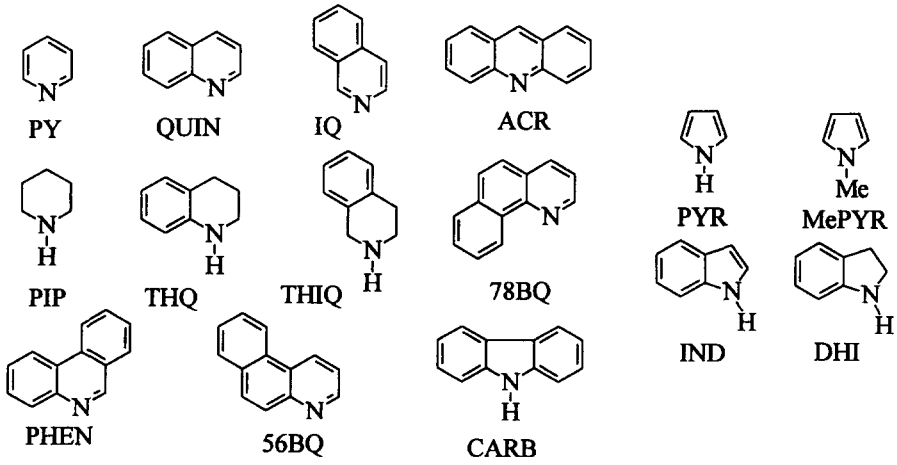

Fig. 1. Model *N*-heterocyclic substrates subject to HDN catalysis.

siderable interest because the preferred substrate coordination mode is expected to dictate the extent and selectivity of ring hydrogenation *and* because nitrogen heterocycles are known to inhibit other desirable hydrotreating reactions [5]. Yet, only a handful of studies have attempted to correlate heterocycle hydrogenation with substrate-metal binding interactions [9,21–30] and even fewer have attempted to relate binding mode to reactivity towards C—N bond cleavage [30–37]. These studies will be described below. Figure 2 depicts possible pyridine and quinoline bonding modes, all of which have been discussed with respect to HDN and many of which are known in isolable complexes.

Observed bonding modes of pyridine (and its derivatives) include the $\eta^1(N)$ [38,39], the $\eta^6(\pi\text{-}N)$ [40–46], the recently discovered $\eta^2(N,C)$ [32,47–51] and $\eta^2(C,C)$ [52,53] structures, and the very rare $\mu\text{-}\eta^1(N)$ [54,55] mode. Furthermore, when considering the bonding modes of *polyaromatic* compounds such as quinoline, the $\eta^6(\pi\text{-}C)$ [56–58] and an $\eta^2(C,C)$ mode involving the benzene ring become possible, although only the $\eta^1(N)$ [30,38,39,56–58], $\eta^6(\pi\text{-}C)$ [56–58] and $\eta^2(N,C)$ [30,32] modes have been described, Fig. 2. There are also many examples of both η^5-pyrrole and deprotonated η^5-pyrrolyl complexes of the transition metals [59–61], as well as η^1-pyrrolyl species [62,63], not shown in Fig. 2. In addition to the above binding modes of nitrogen heterocycles in mononuclear complexes, Rosenberg [64–67], Adams [68–71], Laine [72,73] and others have demonstrated a plethora of binding modes in a variety of unsaturated and partially hydrogenated nitrogen heterocycles, as well as metallated forms of these ligands, in trinuclear clusters. Finally, we call attention to an intriguing $\mu\text{-}\eta^1(N)$ mode in which a pyridine bridges two Mo centers using its nitrogen atom only [54,55]. This compound is especially significant since the molybdenum is in a sulfur-rich environment. The only characterized example of $\mu\text{-}\eta^1(N)$ bonding occurs in the Mo^V pyridine complex $Mo_2O_2[S_2P(OPr^i)_2]_2(\mu\text{-}O)(\mu\text{-}S)[\mu\text{-}\eta^1(N)\text{-}NC_5H_5]$ (**1**) [54,55] prepared by simple pyridine coordination to $Mo_2O_2[S_2P(OPr^i)_2]_2(\mu\text{-}O(\mu\text{-}S)$. $Mo_2O_2[S_2P(OPr^i)_2]_2(\mu\text{-}O)(\mu\text{-}S)$ also reacts with pyridazine to form the μ,η^2 structure **2** shown here.

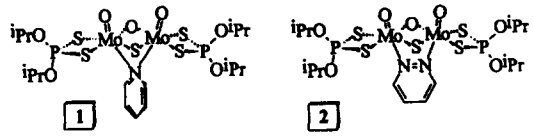

Prior to Wolczanski's discovery of the $\eta^2(N,C)$-pyridine complex $[(\eta^2(N,C)\text{-}NC_5H_5]Ta(silox)_3$ (silox = $OSiBu^t_3$) [47] and our later report of a similar derivative $[\eta^2(N,C)\text{-}2,4,6\text{-}NC_5Bu^t_3H_2]Ta(OAr)_2Cl$ [50], the $\eta^1(N)$- and $\eta^6(\pi\text{-}N)$-bound heterocycles were the most often discussed with regard to substrate interactions with the CoMoS active site [5,74] and most homogeneous studies have also centered around these bonding modes. For example, Fish and coworkers have examined soluble Rh and Ru cyclopentadienyl complexes and demonstrated that heterocycle $\eta^1(N)$ bonding appears to be preferred over $\eta^6(\pi\text{-}N)$ bonding in the absence of steric constraints [24–27,56–58]. These systems have also manifested an intriguing $\eta^1(N) \rightarrow \eta^6(\pi\text{-}N)$ rearrangement [41] (that may involve a transient η^4 intermediate [58]), however, $\eta^1(N)$ binding appears to be a prerequisite for ring hydrogenation [24–27,56–58]. These studies are described in more detail below. The $\eta^2(N,C)$ bonding mode appears to be particularly relevant to HDN, since it has recently been discovered to activate a heterocycle to C—N scission [32–34,36,37]. Wolczanski has reported molecular orbital calculations on the model compound $[(\eta^2(N,C)\text{-}NC_5H_5]Ta(OH)_3$ and has determined that the $\eta^2(N,C)$ coordination mode is preferred when pyridine binds to d^2 $Ta(OH)_3$ because it avoids the high-energy, filled $Ta(OH)_3$ d_{z^2}-pyridine $N(\sigma)$ orbital interaction that would arise in the $\eta^1(N)$-bonded complex, and because the pyridine can function as a π-acceptor in the $\eta^2(N,C)$ mode, thereby allowing the metal to attain its highest oxidation state [48]. These electronic features result in a "metallaaziridine" [75–78] structure of $[(\eta^2(N,C)\text{-}NC_5H_5]Ta(silox)_3$ and $[\eta^2(N,C)\text{-}2,4,6\text{-}NC_5Bu^t_3H_2]Ta(OAr)_2Cl$ in which a 1,3-diene-like π-electron localization and an interruption of pyridine aromaticity are observed.

Only a few heterogeneous catalytic studies have discussed possible substrate binding modes. Many years ago Adkins described an enhancement in the hydrogenation rate of 2,6-dimethylpyridine over that of pyridine with Raney Ni, presumably indicating an $\eta^6(\pi)$ mode of interaction or surface π-complex [79]. However, 5,6-benzoquinoline (56BQ) has been shown to hydrogenate faster than 7,8-benzoquinoline (78BQ) on a sulfided NiW/Al_2O_3 catalyst [5], suggesting the opposite (see Fig. 1). Other bonding modes and substrate–catalyst interactions that have been dis-

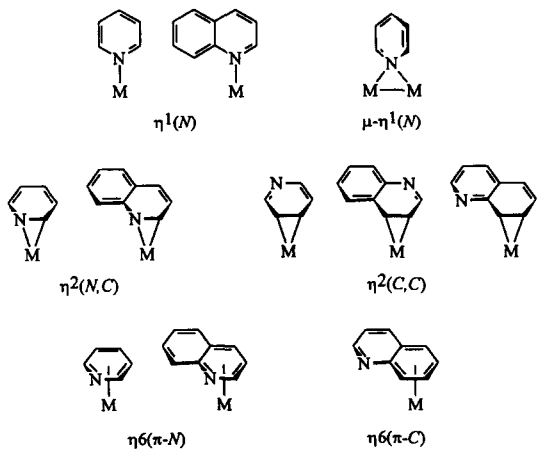

Fig. 2. Possible bonding models in pyridine- and quinoline-transition metal complexes.

cussed are typically based upon analogies with the hydrogenation of aromatic compounds on metals in which a "π to σ" dissociative mechanism or "slip" is proposed [80]. For example, Ho has suggested a π-complex that "slips" to a reactive "σ-complex" [an $\eta^1(C)$ aromatic, not σ-aryl], which is hydrogenated by adjacent —SH groups on the surface [5]. This proposal is consistent with the notion that hydrogen may be dissociatively bound to *sulfur* in the form of sulfhydryl groups at the active site [10,11]. Perhaps the most significant substrate–catalyst discussion relevant to our studies was presented by Cossee who considered π-bonding of a heterocycle in view of a backbonding model from a relatively electron-rich molybdenum site into empty orbitals on the aromatic compound [81]. Thus, if the metal center can be reduced to any oxidation state $d^{n>0}$ (which has been proposed to occur by electron transfer from the cobalt promoter [12]), then population of an empty π^*-orbital on the aromatic compound will interrupt aromaticity and lower the activation energy to hydrogenation.

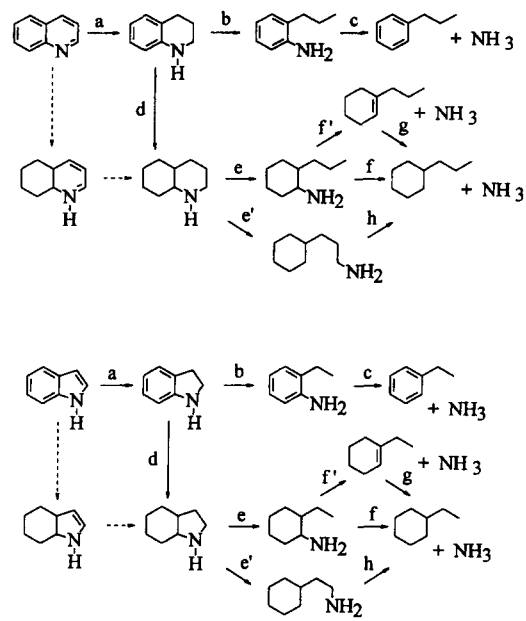

Scheme 1.

4. *General HDN reaction scheme*

It is convenient to discuss heterocycle HDN in terms of the rather rapid hydrogenation steps and the slower C—N hydrogenolysis steps [3,5]. Quinoline is a prototypical HDN substrate that has proved particularly valuable in HDN model studies. It has been shown—primarily on the basis of product analyses—that over a range of conditions it is necessary to hydrogenate *both* the heterocyclic and carbocyclic rings in order to cleave both C—N bonds of quinoline [5,6,82–86]. Therefore, while it is tenuous to form generalizations from one set of substrates, catalysts, and conditions to another, the collective evidence points to general quinoline and indole HDN reaction schemes shown in Scheme 1 [2,8,9].

The most efficient and selective method of quinoline HDN involves the a → b → c pathway, in which the carbocyclic ring is not hydrogenated. This path represents a considerable savings in hydrogen and therefore provides a lower cost and higher quality (higher octane) product. However, the quinoline hydrogenation data suggest that *most* of this substrate undergoes HDN along the a → d → e → f pathway (perhaps involving f′ → g steps), where the carbocycle is also hydrogenated *before* C—N bonds are cleaved [2,87]. In either case, the most facile step is hydrogenation of the heterocycle (step a), therefore, quinoline HDN invariably involves the intermediacy of tetrahydroquinoline, just as indole HDN proceeds *via* indoline. Kinetic studies suggest [21–23,82,88] that the dashed lines of Scheme 1 are not primary pathways for quinoline HDN.

5. C—N *bond scission mechanisms*

While the *hydrogenation* of pyridine rings is comparatively facile under standard HDN conditions, the subsequent C—N bond *hydrogenolysis* reactions are considerably more difficult [8,9,21–23,87]. Since C—N bond cleavage is typically rate-limiting [82–85,89–93], the mechanistic details surrounding this reaction are of singular importance to understanding and improving HDN, especially since the metal's role in promoting this reaction remains unresolved [5]. Studies of thiophene HDS have afforded several well-characterized C—S bond-scission reactions [94–102], but analogous model reactions of *N*-heterocycles are rare. In addition, the greater C—N bond energies as compared with C—S bonds (by 3–9 kcal mol^{-1}) [10] generally make HDN less efficient than HDS catalysis under most conditions [1,2].

Satterfield and coworkers have established that H_2S (formed in HDS reactions) *enhances* the rate of quinoline HDN [84,90–93]. These observations, and those from other groups [83,86], have led to the proposal that either a Hofmann elimination (HE), with SH^- serving as base, or a nucleophilic substitution (SN), with SH^- acting as nucleophile, are the principal mechanisms of C—N bond scission, Scheme 2 [5–8,85,90]. Unfortunately, few deliberations in the catalysis literature consider the participation of a metal center in discussing C—N bond scission mechanisms. Prior to our initial report [31], the few examples of *metal-mediated* C—N bond scissions were limited to aliphatic amine substrates in systems not easily amenable to study. Thus, Laine [103,104], Adams [68,69,71] and Rosenberg [105] have all uncovered C—N scission products at transition metal clusters, suggesting that coordination of the heterocycle is necessary to effect C—N cleavage [7,8,89,103,106]. Several subsequent examples of metal-mediated C—N scissions have been reported [68,69,71,107,108].

Early on in the C—N scission debate, Laine proposed nucleophilic substitution mechanisms (based on H_2S-promoted bond cleavage reactions [109–111]) as outlined in Scheme 2 for C—N bond scission in piperidine [7]. A central feature of this proposal is the participation of an $\eta^2(N,C)$ piperidyl *amine* complex (**3** of Scheme 2) that is formed at the catalytic site. If the subsequent C—N bond cleavage results from hydride transfer to Cα, then formation of a ring-opened *amido* complex occurs. Whether the nature of the migrating hydrogen ligand in Laine's proposal is more hydridic $H^{\delta-}$ or acidic $H^{\delta+}$ throughout migration could not be specifically addressed. This proposal is consistent with Satterfield's evidence that the H_2S rate enhancement effect occurs *in the* C—N *bond cleavage step*, rather than the hydrogenation steps [93,112].

As suggested in Scheme 2, an examination of HE *vs* SN pathways in classic organic mechanisms reveals that saturation and sp^3 hybridization at the carbon α to nitrogen are required for C—N scission by a nucleophilic substitution (SN) mechanism, while saturation at *both* Cα and Cβ is required to effect C—N scission by a Hofmann elimination (HE). Thus, for *quinoline*, hydrogenation of the *carbocyclic* ring of 1,2,3,4-tetrahydroquinoline (THQ) is required to cleave both C—N bonds of this compound by *either* mechanism, a feature consistent with propylcyclohexane as the principle product of quinoline HDN under a variety of conditions, Scheme 3 [113]. Perot and coworkers have used this saturation difference between HE and SN reactions to distinguish between these pathways in the C—N cleavage reactions of tetrahydro*isoquinoline* and thereby have obtained strong evidence that the SN mechanism is the major C—N cleavage pathway in tetrahydro-*isoquinoline* (THIQ) HDN, Scheme 4 [85,113]. Thus,

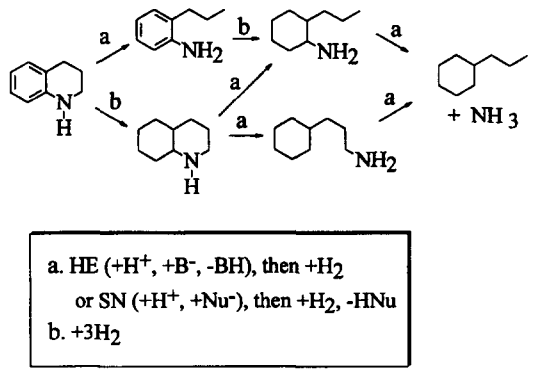

Scheme 3.

the formation of any 2-ethyltoluene in tetrahydroisoquinoline HDN must arise from an SN mechanism, based upon the sp^3 hybridization requirement described above, whereas 1-ethyl-2-methylcyclohexane will arise from HE chemistry, Scheme 4. The Perot experiment revealed that under the same conditions that quinoline reacts to give primarily THQ, tetrahydroisoquinoline undergoes HDN to afford primarily 2-ethyltoluene, *consistent with an SN mechanism* of C—N bond cleavage. Perot notes that substitutions at the carbon α to nitrogen results in changes in the HDN product distribution, perhaps signalling a change in mechanism for the C—N scission step [85].

HOMOGENEOUS HYDRODENITROGENATION MODEL STUDIES

Despite the significant advances described above, problems with the current practice of HDN catalysis

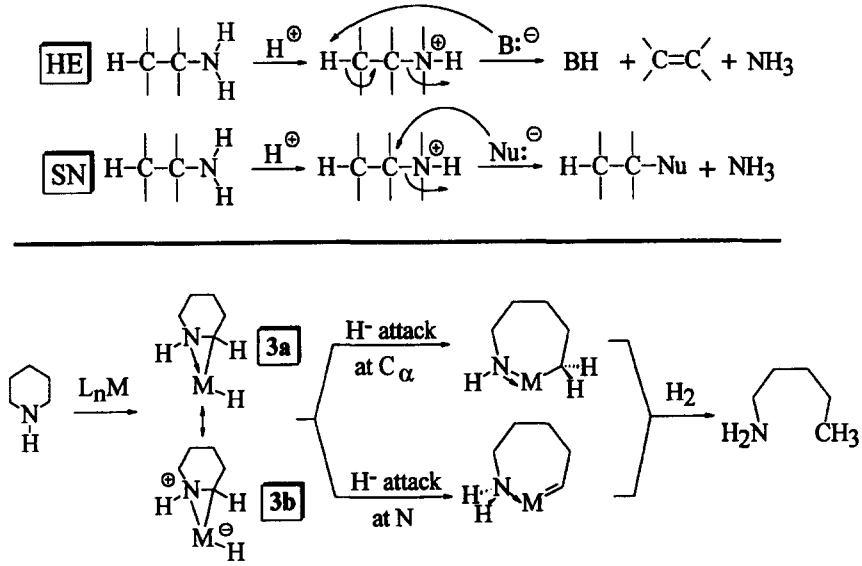

Scheme 2.

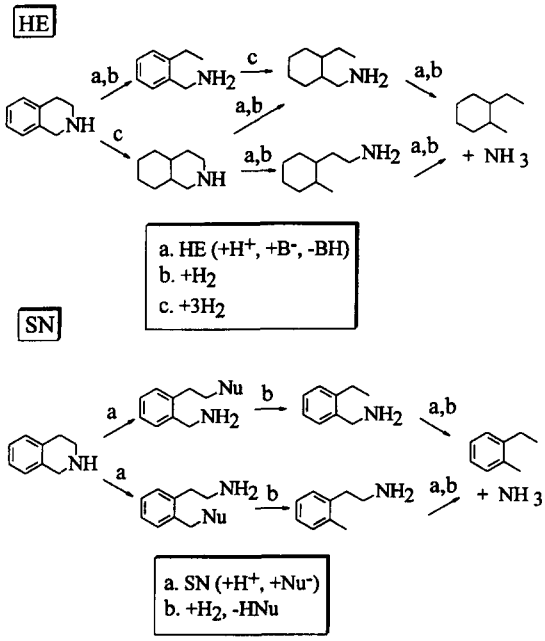

Scheme 4.

remain. Hydrogen consumption represents a major cost of hydrotreating and HDN is a principal H_2 consumer since achieving nitrogen removal typically occurs only after complete hydrogenation of all aromatic rings of the heterocycle. As a result, the HDN reaction network is very nonselective in nature and results in a lower quality fuel product. Although HDN, HDS, HDO, etc. are all carried out simultaneously during hydrotreating, this process is typically optimized for HDS, making nitrogen removal less efficient than sulfur removal. Finally, because our fundamental mechanistic understanding of HDN is crude, improvements in current HDN technology and developing new HDN catalysts are largely empirically based. Significant, unsettled questions in HDN catalysis include how the strong C—N bonds in the heterocyclic compounds are cleaved and to what extent the metal sulfide site mediates this reaction. This section will outline homogeneous model studies that attempt to address these questions.

1. *Substrate binding and hydrogenation in homogeneous systems*

Both the binding modes and hydrogenation behavior of heteroaromatic compounds have been examined in an elegant series of studies by Fish and coworkers using soluble rhodium- and ruthenium-heterocycle complexes [24–27,56–58]. If steric restrictions in these complexes are not too demanding, N-bonding [$\eta^1(N)$] appears to be more favorable than $\eta^6(\pi)$ bonding. However, reduction of the N-ring is clearly a function of the bonding mode since $\eta^1(N)$ coordination appears to be a requirement for ring hydrogenation [24–27,56–58]. Moreover, to be catalytically active, rhodium complexes of the type $[(\eta^5\text{-}C_5Me_5)Rh]^{2+}$ must have two replacable ligands, i.e. have the general form $[(\eta^5\text{-}C_5Me_5)Rh(\eta^1(N)\text{-heterocycle})L_2]^{2+}$. The product of selective quinoline hydrogenation, 1,2,3,4-tetrahydroquinoline (THQ), has been found to bind $\eta^6(\pi\text{-}C)$ to $[(\eta^5\text{-}C_5Me_5)_2Rh]^{2+}$ [57], a fact that may account for its not being further hydrogenated under mild conditions and for its adverse effect on the hydrogenation rate of quinoline itself [25].

Fish has also used deuterium gas experiments to study the regioselectivity of quinoline hydrogenation using the rhodium catalyst precursors $Rh(PPh_3)_3Cl$ [25] and $[(\eta^5\text{-}C_5Me_5)Rh(NCMe)_3]^{2+}$ [27]. The observed selectivity of deuteration is presented in Scheme 5 and summarized as follows: (1) the 1,2-N=C bond was rapidly and *reversibly* deuterated (NMR revealed *ca* 1.5 d at position 2); (2) this step was followed by 3,4-C=C bond deuteration (*ca* 1 d each at these positions); and finally, (3) H/D exchange occurred on the aromatic ring in positions 6- and 8-, most likely reflecting C—H bond metallation at the Rh^{3+} center under the hydrogenation conditions. The fact that the heterogeneous, supported form of $Rh(PPh_3)_3Cl$ reacted with the same regioselectively and with excellent conversions supports the validity of these homogeneous systems as relevant HDN models [114].

The hydrogenation of five- *vs* six-membered rings is expected to occur *via* different metal–substrate interactions and one possible model for this hydrogenation exists in the deuteration experiments of benzothiophene using $[(\eta^5\text{-}C_5Me_5)Rh(NCMe)_3]^{2+}$ [27]. In this experiment, Fish found stereoselective 2,3-C=C *cis*-deuteration under kinetic conditions and suggests that η^2- or η^3-binding (rather than initial η^1 as in the nitrogen substrates) is responsible. (Recall that the thermodynamic binding of benzothiophene to $[(\eta^5\text{-}C_5Me_5)Rh]^{2+}$ is η^6 [115,116].) Laine and coworkers have also studied the heterocycle binding and the selectivity of hydrogenation of nitrogen heterocycles in cluster complexes [72,73,89,103].

Our efforts have been directed towards highly electrophilic, mononuclear complexes of the early metals, especially tantalum, that bind nitrogen heterocycles in both the $\eta^1(N)$ and $\eta^2(N,C)$ modes. Thus, the complexes $[\eta^1(N)\text{-QUIN}]Ta(OAr)_3Cl_2$ (**4**), $[\eta^1(N)\text{-6MQ}]Ta(OAr)_3Cl_2$ (**5**) and $[\eta^1(N)\text{-6MQ}]Ta(OAr)_2Cl_3$ (**6**) (where OAr = O-2,6-$C_6H_3Pr^i_2$, QUIN = quinoline and 6MQ = 6-methylquinoline) are prepared in quantitative yield from $Ta(OAr)_3Cl_2(OEt_2)$

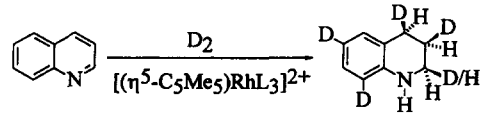

Scheme 5.

or $Ta(OAr)_2Cl_3(OEt_2)$ and QUIN or 6MQ [30]. Upon the *rapid*, two-electron reduction of these complexes, an $\eta^1(N) \rightarrow \eta^2(N,C)$ bonding rearrangement is effected and the d^2 species $[\eta^2(N,C)$-QUIN]$Ta(OAr)_3$ (**7**), $[\eta^2(N,C)$-6MQ]$Ta(OAr)_3$ (**8**) and $[\eta^2(N,C)$-6MQ]$Ta(OAr)_2Cl(OEt_2)$ (**9**) can be isolated in moderate yields, although these reactions are not always reproducible, Scheme 6. Alternatively, $[\eta^2(N,C)$-6MQ]$Ta(OAr)_2Cl(OEt_2)$ (**9**) can be prepared from $(\eta^6\text{-}C_6Me_6)Ta(OAr)_2Cl$ (**10**) and 6MQ, but a simple pyridine complex such as $[\eta^2(N,C)\text{-}NC_5H_5]Ta(OAr)_2Cl(OEt_2)$ is *not* isolable by this route.

We emphasize that the isolation of the bis (aryloxide) species $[\eta^2(N,C)$-6MQ]$Ta(OAr)_2Cl(OEt_2)$ (**7**) must be accomplished by the *rapid, two-electron* reduction of the d^0 starting complex. If the *second* electron transfer in this reduction is not carried out rapidly enough, the intermediate d^1 complex acts as an effective scavenger of 6MQ from solution and the stable, six-coordinate Ta^{IV} complex $[\eta^1(N)$-6MQ$]_2Ta(OAr)_2Cl_2$ is isolated. Accordingly, the d^1 compound $[\eta^1(N)$-6MQ$]_2Ta(OAr)_2Cl_2$ (**11**), as well as related species such as the pyridine adduct $[\eta^1(N)$-py$]_2Ta(OAr)_2Cl_2$, are available from the one-electron reduction of $Ta(OAr)_2Cl_3(OEt_2)$ in the presence of the corresponding heterocycle, Scheme 6. However, complex **11** is *not* readily converted to its $\eta^2(N,C)$ analog **9** by further reduction, therefore, if another heterocycle coordinates *prior* to the second electron transfer, this reduction is exceedingly difficult. Based upon our observations, the sequence of reactions leading to d^0, d^1 and d^2 heterocyclic adducts is proposed in eqs (1)–(5), where the 6MQ complexes specifically have been isolated in each oxidation state. These observations are consistent with the generation of an intermediate d^1 complex $[\eta^1(N)$-6MQ$]Ta(OAr)_2Cl_2(OEt_2)_n$, where $n = 0$ or 1, that partitions between two further reactions: either another one-electron reduction, eq. (4), or coordination of another 6MQ ligand, eq. (5) [30].

$$Ta(OAr)_2Cl_3(OEt_2) + 6MQ \rightleftarrows [\eta^1(N)\text{-6MQ}]Ta(OAr)_2Cl_3 + Et_2O \quad (1)$$

$$[\eta^1(N)\text{-6MQ}]Ta(OAr)_2Cl_3 + e^- \rightarrow [\eta^1(N)\text{-6MQ}]Ta(OAr)_2Cl_2 \quad (2)$$

$$[\eta^1(N)\text{-6MQ}]Ta(OAr)_2Cl_2 + Et_2O \rightleftarrows [\eta^1(N)\text{-6MQ}]Ta(OAr)_2Cl_2(OEt_2) \quad (3)$$

$$[\eta^1(N)\text{-6MQ}]Ta(OAr)_2Cl_2(OEt_2)_n + e^- \rightarrow [\eta^2(N,C)\text{-6MQ}]Ta(OAr)_2Cl(OEt_2) \quad (4)$$

$$[\eta^1(N)\text{-6MQ}]Ta(OAr)_2Cl_2(OEt_2)_n + 6MQ \rightarrow [\eta^1(N)\text{-6MQ}]_2Ta(OAr)_2Cl_2 \quad (5)$$

Structural studies of $[\eta^2(N,C)$-6MQ]$Ta(OAr)_3(PMe_3)$ and $[\eta^2(N,C)$-6MQ]$Ta(OAr)_2Cl(OEt_2)$ (**9**), Fig. 3, indicate an interruption of aromaticity to the heterocyclic ring, *but not the carbocycle*, when bound in this fashion. Accordingly, under mild hydrogenation conditions, the only ligands that are hydrogenated are those bound in the $\eta^2(N,C)$ mode to a d^2 metal and the only ring that is hydrogenated in these ligands is the heterocycle. For example, hydrogenation of $[\eta^2(N,C)$-QUIN]$Ta(OAr)_3$ (**7**) under mild conditions (room temperature, 125 psi H_2) afford 1,2,3,4-tetrahydroquinoline (THQ) as the principle hydrogenation product. Under these conditions, neither d^0 $[\eta^1(N)$-QUIN]$Ta(OAr)_3Cl_2$ (**4**), d^0 $[\eta^1(N)$-6MQ]$Ta(OAr)_2Cl_3$ (**6**), d^1 $[\eta^1(N)$-6MQ$]_2Ta(OAr)_2Cl_2$ (**11**), nor free quinoline is hydrogenated. Further-

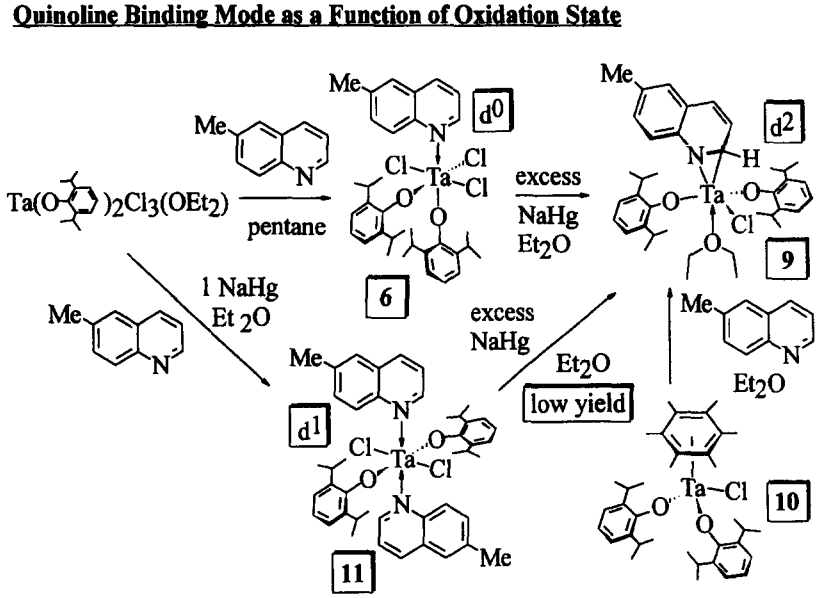

Scheme 6.

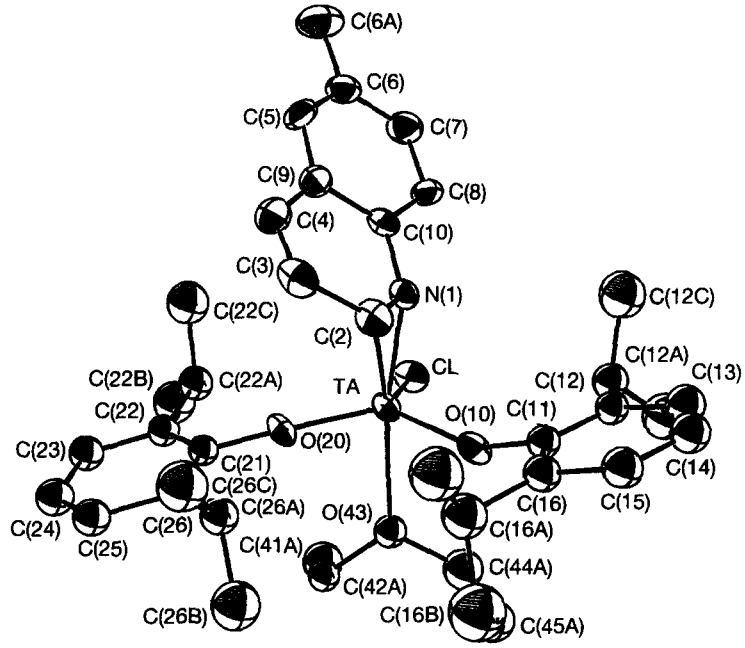

Fig. 3. Molecular structure of $[\eta^2(N,C)\text{-6MQ}]Ta(OAr)_2Cl(OEt_2)$ (**9**) (6MQ = 6-methylquinoline, Ar = 2,6-$C_6H_3Pr^i_2$).

more, in the hydrogenation of $[\eta^2(N,C)\text{-QUIN}]Ta(OAr)_3$, no decahydroquinoline is observed.

2. *Carbon–nitrogen bond cleavage in* η^2(N,C)-*pyridine complexes*

Metal-mediated C—N bond scissions have typically been limited to aliphatic amine substrates in systems not easily amenable to study [69,70,103–105,117]. In the course of our studies of alkyne cycloaddition chemistry [51], we prepared the η^2-pyridine complex $[\eta^2(N,C)\text{-}2,4,6\text{-}NC_5Bu^t_3H_2]Ta(OAr)_2Cl$ (**12**), a species that also exhibits a "metallaaziridine" structure and can be considered a model substrate → catalyst adduct related to $[\eta^2(N,C)\text{-QUIN}]Ta(OAr)_3$ (**7**) and $[\eta^2(N,C)\text{-6MQ}]Ta(OAr)_2Cl(OEt_2)$ (**9**) [31–33]. Upon reacting $[\eta^2(N,C)\text{-}2,4,6\text{-}NC_5Bu^t_3H_2]Ta(OAr)_2Cl$ (**12**) with 1 equiv. of $LiBEt_3H$, red crystalline **13** can be isolated in moderate yield after appropriate workup, Scheme 7. The NMR spectra of **13** are consistent with hydride addition occurring at the metal-bound carbon of the $\eta^2(N,C)$-pyridine ligand, however, an X-ray structural study of this complex provided the dramatic evidence that the C—N bond of the $\eta^2(N,C)$-pyridine ligand in **12** had been cleaved upon hydride addition, Fig. 4.

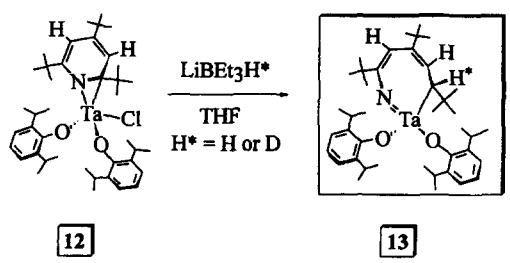

Scheme 7.

The disconnection between the N and C(1) of the former pyridine ligand and the resulting, seven-membered metallacyclic structure of $Ta(=NCBu^t=CHCBu^t=CHCHBu^t)(OAr)_2$ (**13**) are unambiguous, confirming that net hydride addition has occurred to the pyridine C(1). Thus, in the metallaaziridine description [75–78] of $[\eta^2(N,C)\text{-}2,4,6\text{-}NC_5Bu^t_3H_2]Ta(OAr)_2Cl$ (**12**), the former *amido* nitrogen [48] has been transformed into a formal *imido* linkage upon

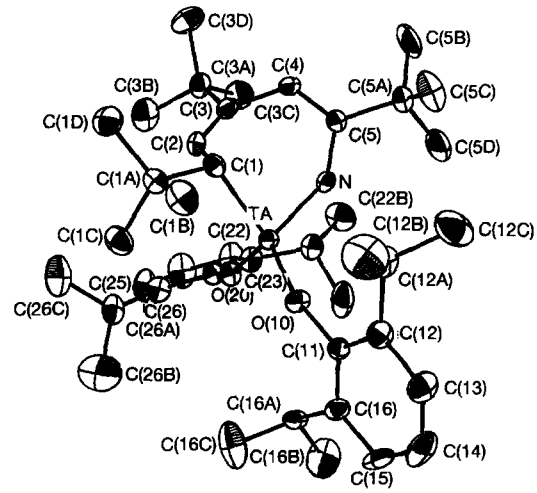

Fig. 4. Molecular structure of $Ta(=NCBu^t=CHCBu^t=CHCHBu^t)(OAr)_2$ (**13**) (Ar = 2,6-$C_6H_3Pr^i_2$).

hydride attack, as depicted in Scheme 7. The formation of the strong metal–ligand multiple bond in **13** no doubt represents a major driving force for this reaction, since a strong C—N bond is cleaved in this process.

Following this discovery, we set out to uncover the mechanistic details of this important C—N bond scission reaction. Of the possible scenarios that could account for the **12** → **13** conversion, perhaps the most significant question to address is the extent to which the metal center mediates the reaction. The most simple mechanism involves a direct, *exo* hydride attack on the bound carbon of the pyridine complex, Scheme 8. Nucleophilic attack of the hydride at the metal to form an unstable hydride complex, followed by an *endo* hydride transfer from the metal to the pyridine ligand also represents a viable pathway for C—N bond scission, Scheme 8. An examination of the molecular structure of **13** reveals that the hydride has apparently added to the face of the pyridine ligand directed away from the metal center, Fig. 4. Thus, it *appears* that an *exo* mechanism for hydride transfer to the pyridine ligand has occurred. However, we note that *endo* attack cannot be ruled out from the molecular structure of **13** alone, as simple rotation about the Ta—C(1) bond and the Ta—N—C(5) linkage of the metallacycle of an *endo*-addition product, brought about by an "envelope ring flip", would result in an apparent *endo*-addition structure. This process is represented for both enantiometers of **13** in Scheme 9.

No identifiable intermediates could be detected spectroscopically in the complex reaction of **12** with $LiBEt_3H$, and all attempts to prepare the purported $\eta^2(N,C)$-pyridine-hydride complex, $[\eta^2(N,C)$-2,4,6-$NC_5Bu^t_3H_2]Ta(OAr)_2H$ by other routes led to either uncharacterizable products or no reaction. Finally, our attempts to address this question of *endo- vs exo*-hydride attack in Scheme 8 led us to examine the reactions of $[\eta^2(N,C)$-2,4,6-$NC_5Bu^t_3H_2]Ta(OAr)_2Cl$ (**12**) with carbon nucleophiles, which was considered an attractive prospect to establish the regioselectivity of attack.

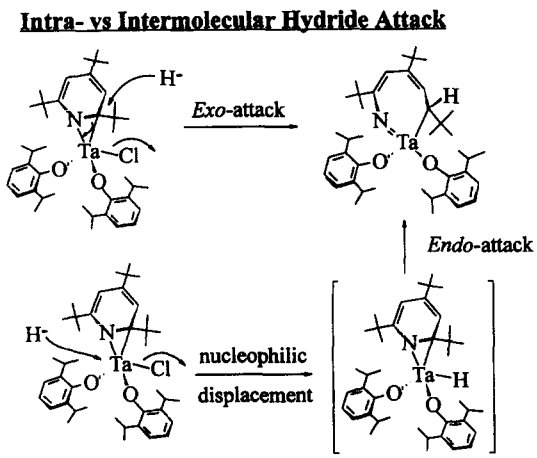

Scheme 8.

The reactions of **12** with alkyl lithium or Grignards afford the alkyl compounds $[\eta^2(N,C)$-2,4,6-$NC_5Bu^t_3H_2]Ta(OAr)_2R$ [R = Me (**14**), Et (**15**), Pr^n (**16**), Bu^n (**17**) and CH_2SiMe_3 (**18**)], affording direct evidence that the metal center is the initial site of nucleophilic attack, Scheme 10. While reaction at the metal center is highly significant, we subsequently discovered that compounds **14**–**17** constitute the *kinetic* products of this system. Thus, upon thermolysing these species we observe the onset of two reactions: first a "ring-rocking" process ensues in which pyridine *ortho* carbons alternately coordinate and then dissociate from the metal, as suggested in Scheme 10; and second, at higher temperatures, an *alkyl migration* from metal to ligand occurs in **14**–**17** (but not **18**) and the ring-opened, C—N bond cleavage compounds $Ta(=NCBu^t=CHCBu^t=CHCBu^tR)(OAr)_2$[R = Me (**19**), Et (**20**), Pr^n (**21**), Bu^n (**22**)] are formed, Scheme 11 [33].

Although the C—N cleavage reactions of Scheme 11 would appear to be intramolecular alkyl transfers, these results alone cannot rule out an *inter*molecular alkyl transfer to the *exo* position of another, nearby η^2-pyridine ligand in a bimolecular reaction. This determination is central to understanding the role of the transition metal in mediating C—N bond cleavage and therefore in addressing a fundamental question surrounding HDN. To examine this process, a simple crossover experiment was carried out which takes advantage of the three-bond $^3J_{CH}$ coupling observed for the H(2) proton in the ^1H NMR spectrum of $Ta(=NCBu^t=CHCBu^t=CHCBu^{t13}CH_3)(OAr)_2$ (**19**-^{13}C) that arises from thermolysing $[\eta^2(N,C)$-2,4,6-$NC_5Bu^t_3H_2]Ta(OAr)_2(^{13}CH_3)$ (**14**-^{13}C), Scheme 11. Thus, an equimolar mixture of $[\eta^2(N,C)$-2,4,6-$NC_5Bu^t_3D_2]Ta(OAr)_2Me$ (**14**-d_2) and $[\eta^2(N,C)$-2,4,6-$NC_5Bu^t_3H_2]Ta(OAr)_2(^{13}CH_3)$ (**14**-^{13}C) was thermolysed (C_6D_6, sealed tube, 120°C, 4 h) and the resulting ring cleaved products observed by ^1H NMR, Scheme 12. The H(2) resonance of the cleavage product appears as a doublet *only* in the ^1H NMR spectrum of this reaction, implying that *only* $Ta(=NCBu^t=CDCBu^t=CDCBu^tMe)(OAr)_2$ (**19**-d_2) and $Ta(=NCBu^t=CHCBu^t=CHCBu^{t13}CH_3)(OAr)_2$ (**19**-^{13}C) are present in the sample; *none* of the possible crossover products $Ta(=NCBu^t=CHCBu^t=CHCBu^tMe)(OAr)_2$ (**19**) or $Ta(=NCBu^t=CDCBu^t=CDCBu^{t13}CH_3)(OAr)_2$ (**19**-^{13}C,d_2) is detected. Similarly, thermolysing an equimolar mixture of $[\eta^2(N,C)$-2,4,6-$NC_5Bu^t_3H_2]Ta(OAr)_2Me$ (**14**) and $[\eta^2(N,C)$-2,4,6-$NC_5Bu^t_3D_2]Ta(OAr)_2(^{13}CH_3)$ (**14**-^{13}C,d_2) in the reverse crossover experiment affords *only* $Ta(=NCBu^t=CHCBu^t=CHCBu^tMe)(OAr)_2$ (**19**) and $Ta(=NCBu^t=CDCBu^t=CDCBu^{t13}CH_3)(OAr)_2$ (**19**-^{13}C,d_2), Scheme 12. The results of these experiments unambiguously demonstrate that methyl

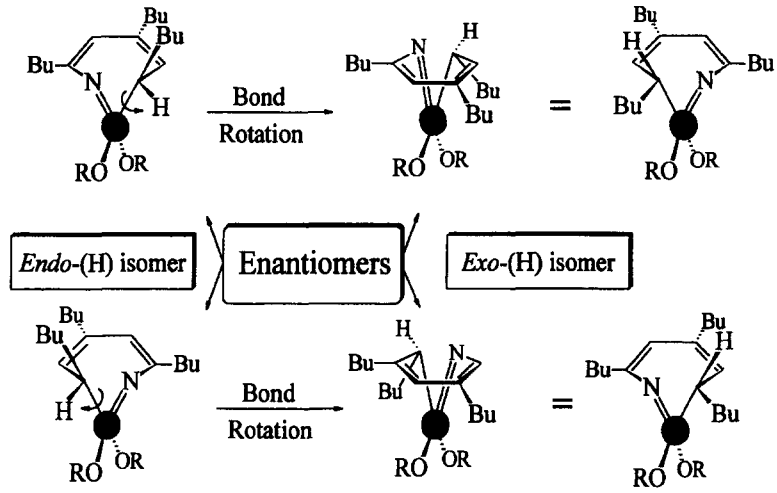

Scheme 9.

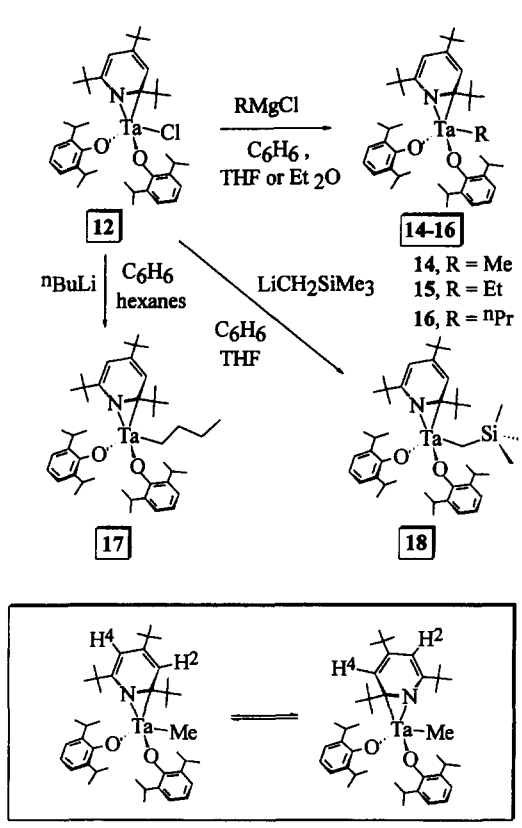

Scheme 10.

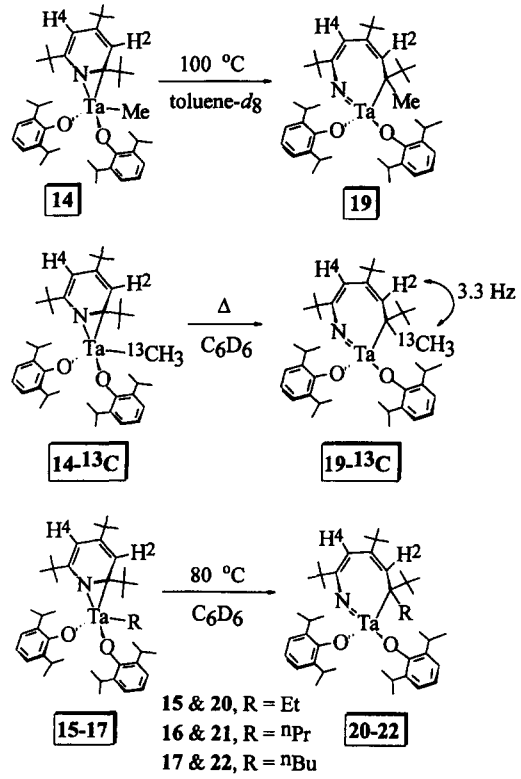

Scheme 11.

migration in the **14** → **19** reaction occurs in an *intramolecular* fashion. Thus, an "envelope ring-flip" of the C—N cleaved, metallacyclic imido product must be operable to account for the isolation of an apparent *exo* addition product that arises from the *endo* addition kinetic product as shown in Scheme 9.

Kinetic studies of the conversion of $[\eta^2(N,C)$-2,4,6-$NC_5Bu^t_3H_2]Ta(OAr)_2Me$ (**14**) to $Ta(=NCBu^t{=}CHCBu^t{=}CHCBu^tMe)(OAr)_2$ (**19**)

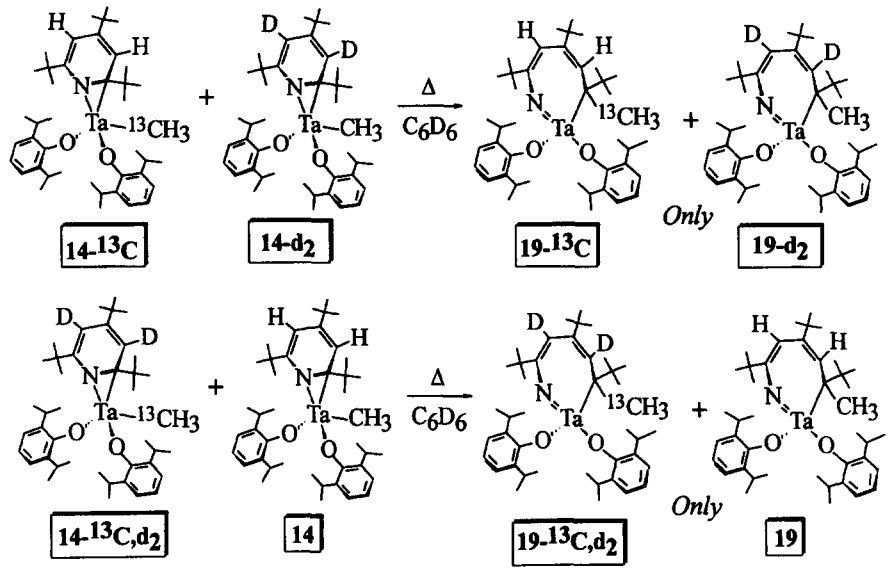

Scheme 12.

by ^{1}H NMR (toluene d_8, 100°C) reveal that the disappearance of **14** obeys first-order kinetics ($R^2 = 0.981$) over greater than three half lives, consistent with the crossover experiments. The reaction is quite slow at this temperature ($t_{1/2} = 8.75$ h) and the C—N bond cleavage product **19** reaches a steady state concentration after approximately one half-life owing to its further degradation under these conditions. The subsequent decomposition process is described below.

Wolczanski and coworkers have uncovered two additional forms of C—N bond scission, both effected at d^2 M(OR)$_3$ (M = Nb, Ta) centers [36,37]. The first of these involves the oxidative addition of the arylamine C—N bond of $H_2NC_6H_4X$ to Ta(silox)$_3$ (silox = OSiBu$^t_3$) to form (silox)$_3$Ta(NH$_2$)(C$_6$H$_4$X). This reaction may also afford the N—H addition product (silox)$_3$Ta(H)(NHC$_6$H$_4$X) depending upon the substituent X [37]. In this reaction, electron-withdrawing substituents on the aryl ring increase the rate of the C—N scission reaction relative to the N—H oxidative addition reaction, therefore, if the metal is highly nucleophilic, sp^3 hybridization at the C—N bond (as in Satterfield's proposals, Scheme 2) may not be necessary. The pyridine C—N bond of [η^2(*N*,*C*)-NC$_5$H$_5$]Nb(silox)$_3$ is subject to cleavage in an unusual reaction shown in eq. (6). Thus, thermolysis of [η^2(*N*,*C*)-NC$_5$H$_5$]Nb(silox)$_3$ (70°C, benzene) affords 0.5 equiv of pyridine and 0.5 equiv of the ring-opened product (silox)$_3$Nb=CH(CH=CH)(CH=CH)N=Nb(silox)$_3$ [36]. The kinetic products are the *cis,cis* and *trans,cis* isomers that subsequently thermolyse to afford the equilibrium mixture of *cis,cis*, *trans,cis*, *trans,trans*, and *cis,trans* in a 6:26:59:9 ratio. Isomerization of the C=C double bond closer to the alkylidene is more facile than isomerization of the double bond closer to the imide.

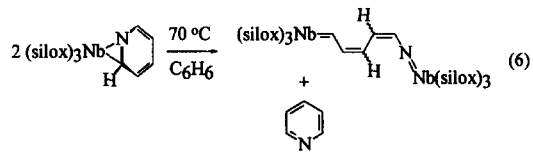

(6)

3. *Mechanistic details of the carbon–nitrogen bond cleavage in an* η^2(N,C)*-pyridine complex: nature of the migrating ligand*

In the same manner that [η^2(*N*,*C*)-2,4,6-NC$_5$Bu$^t_3$H$_2$]Ta(OAr)$_2$Cl (**12**) can be alkylated, **12** also reacts with PhLi to afford the phenyl complex [η^2(*N*,*C*)-2,4,6-NC$_5$Bu$^t_3$H$_2$]Ta(OAr)$_2$Ph (**23**) in moderate yield [34]. The *para*-substituted phenyl derivatives [η^2(*N*,*C*)-2,4,6-NC$_5$Bu$^t_3$H$_2$]Ta(OAr)$_2$(4-C$_6$H$_4$X), where X = OMe (**24**), Me (**25**), Cl (**26**), and CF$_3$ (**27**), are prepared similarly from **12** and the appropriate aryl Grignard or lithium reagent, Scheme 13. Complexes **23**–**27** also undergo aryl migration from metal to ligand upon their thermolysis and the ring-opened compounds Ta[=NCBu^t=CHCBu^t=CHCBu^t(4-C$_6$H$_4$X)](OAr)$_2$, where X = H (**28**), OMe (**29**), Me (**30**), Cl (**31**) and CF$_3$ (**32**) are formed by C—N bond scission, Scheme 14. Kinetic studies of these rearrangements reveal that aryl migration follows clean first-order kinetics, implying an intramolecular, *endo* attack of the migrating aryl group on the pyridine ligand, just as described above for the alkyl complexes [34].

These compounds have allowed a careful mechanistic study of the C—N bond cleavage reaction. Thus, variable-temperature kinetic studies provide activation parameters for [η^2(*N*,*C*)-2,4,6-NC$_5$Bu$^t_3$H$_2$]Ta(OAr)$_2$(4-C$_6$H$_4$OMe) (**24**) → Ta[=NCBu^t=CHCBu^t=CHCBu^t(4-C$_6$H$_4$OMe)](OAr)$_2$ (**29**) re-

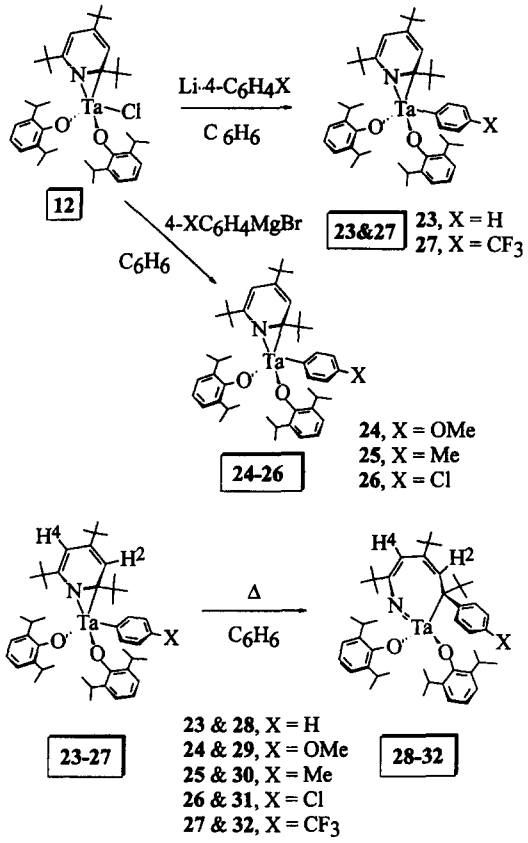

Scheme 13.

Thermolysis of [η²(*N*,*C*)-NC₅ᵗBu₃H₂]Ta(OAr)₂(4-C₆H₄X)

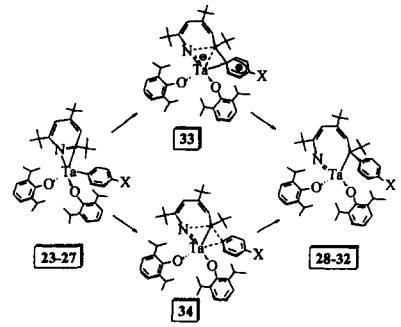

Kinetic Data (80 °C, C_6D_6)

Reaction	X	Rate X 10^6 (s^{-1})	Relative Rate
24→29	OMe	7.4 ± 0.2	1.7
25→30	CH_3	7.0 ± 0.2	1.6
23→28	H	4.3 ± 0.1	1
26→31	Cl	4.3 ± 0.1	1
27→32	CF_3	2.5 ± 0.1	0.6
Hammett Parameter ρ = -0.56 ± 0.10			
24→29	OMe	$\Delta H^{\ddagger}$ = +19.2 ± 1.3 kcal mol^{-1} $\Delta S^{\ddagger}$ = -27 ± 4 cal K^{-1} mol^{-1} $\Delta G^{\ddagger}$(25°C) = +27.3 ± 1.3 kcal mol^{-1}	

Scheme 14.

arrangement of $\Delta H\ddagger = +19.2 \pm 1.3$ kcal mol^{-1} and $\Delta S\ddagger = -27 \pm 4$ cal K^{-1} mol^{-1}, for a $\Delta G\ddagger = +27.3 \pm 1.3$ kcal mol^{-1} at 25°C, suggesting a highly ordered transition state leading to aryl transfer, Scheme 14. The large *entropic* barrier to initiate C—N bond cleavage presumably arises since bond scission occurs from only one of the two $\eta^2(N,C)$ isomers that equilibrate *via* ring rocking, *viz.* a structure with proximate Cα and aryl groups.

A plot of $\log k$ *vs* the Hammett constants σ_p for aryl migration in the $[\eta^2(N,C)$-2,4,6-$NC_5Bu^t_3H_2]Ta(OAr)_2(4\text{-}C_6H_4X)$ series **23–27** gives a reasonably linear fit with $\rho = -0.56 \pm 0.10$. While the *sign* of ρ is in agreement with an electrophilic aromatic substitution at the migrating aryl ligand, the small value of ρ argues against this pathway and against the involvement of the aryl π-framework during migration. Most electrophilic aromatic substitutions that involve Wheland intermediates such as **33** in Scheme 14 are typically characterized by values of ρ from *ca* −2 to −12 [118]. This observation, along with the fact that the alkyl complexes $[\eta^2(N,C)$-2,4,6-$NCBu^t_3H_2]Ta(OAr)_2R$ (**14–17**) undergo a similar ligand migration, also argues against a classic, electrophilic aromatic substitution at the migrating aryl ligand as depicted by **33** [118]. While ligand migration is relatively insensitive to the nature of the *para*-substituent, C—N bond scission by migration of the aryl group as a nucleophile, in particular as a *σ-nucleophile* as suggested by transition state **34,** is nevertheless indicated, Scheme 14. Note that our terminology σ nucleophile (*vs* π nucleophile) is used to distinguish between transition states **33** *vs* **34** in Scheme 14 and should not be confused with the "σ-complex" *vs* "π-complex" terminology to describe intermediates in generalized mechanisms of electrophilic, aromatic substitution. Thus, both structures **33** *vs* **34** represent "σ-complexes" in the classic sense, however, **33** arises from the reactivity of the aryl ligand as a π-nucleophile, while **34** arises from its reactivity as a σ-nucleophile, without involvement of the aryl π-system [34].

4. *Further heterocycle degradation: metallapyridine intermediates in a pyridine decomposition sequence*

While the alkyl complexes $[\eta^2(N,C)$-2,4,6-$NC_5Bu^t_3H_2]Ta(OAr)_2R$ (**14–17**) have been shown to constitute kinetic products of this system, the ring-opened, metallacyclic imido compounds $Ta(=NCBu^t{=}CHCBu^t{=}CHCBu^tR)(OAr)_2$ (**19–22**) have also been identified as unstable kinetic products [33]. For example, upon exhaustive thermolysis of solutions of $[\eta^2(N,C)$-2,4,6-$NC_5Bu^t_3H_2]Ta(OAr)_2Me$ (**14**), the first formed metallacycle $Ta(=NCBu^t{=}CHCBu^t{=}CHCBu^tMe)(OAr)_2$ (**19**) undergoes further decomposition to afford a quantitative yield of orange, air- and moisture-stable **39,** Scheme 15. This species is completely insoluble in

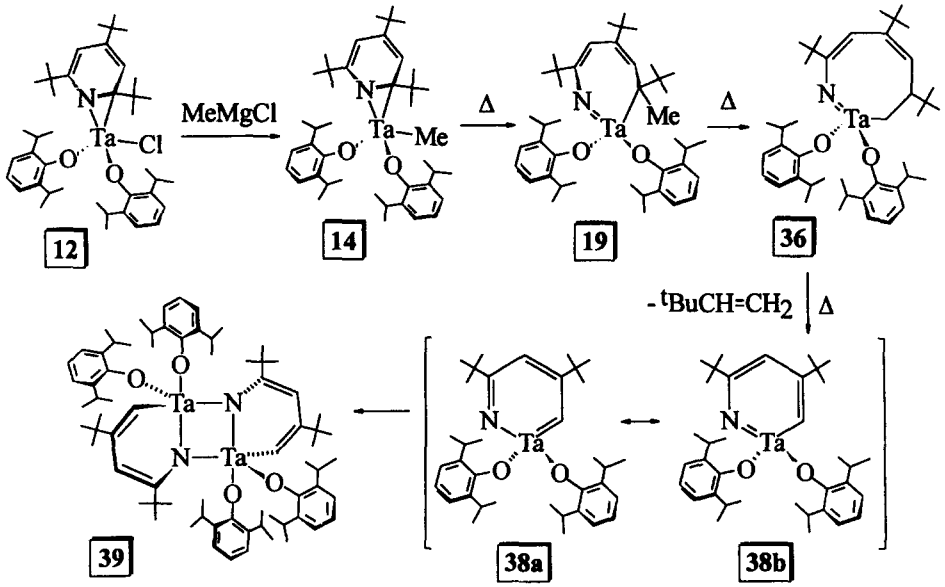

Scheme 15.

most solvents, however, it was possible to grow X-ray quality crystals directly from the **14** decomposition reaction in refluxing benzene. The X-ray structural study of **39** reveals this robust molecule to be a dimer of the formal metallapyridine complex, $[Ta(\mu\text{-}NBu^t{=}CHBu^t{=}CH)(OAr)_2]_2$ (**39**), Scheme 15 and Fig. 5. In the **14** → **19** → **39** conversion, the net loss of 1 equiv. of *tert*-butylethylene per tantalum has apparently occurred and, indeed, monitoring the reaction in a sealed NMR tube (C_6D_6, 110°C) reveals that 0.91 equiv. of $Bu^tCH{=}CH_2$ is formed per equiv.

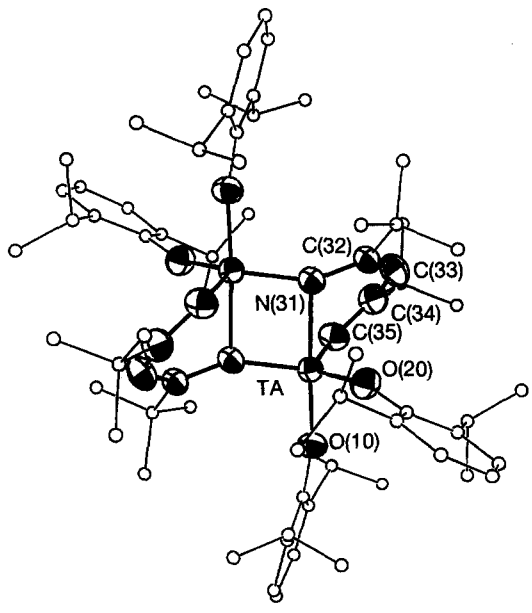

Fig. 5. Molecular structure of $[Ta(\mu\text{-}NBu^t{=}CHBu^t{=}CH)(OAr)_2]_2$ (**39**) (Ar = 2,6-$C_6H_3Pr^i_2$).

of **14** consumed. To determine the source of the *tert*-butylethylene, the labeling experiments presented in Scheme 16 were carried out. These results clearly indicate that the *migrating methyl group* in the **14** → **19** → **39** decomposition serves as the sole source for *all three* olefinic hydrogens of the *tert*-butylethylene produced. Additionally, the ^{13}C-labeling experiment in Scheme 16 demonstrates that the migrating methyl group serves as the sole source of the terminal, methylene carbon of the resulting $Bu^tCH{=}CH_2$.

Having identified the source of the *tert*-butylethylene decomposition product, we set out to establish the mechanism of its formation. Fortunately, the **14** → **39** decomposition is accompanied by the formation of, and then smooth disappearance of, a small concentration of *another* intermediate in the reaction, complex **36,** therefore, the sequence of *observed* compounds for pyridine ring cleavage and degradation is **14** → **19** → **36** → **39,** Scheme 15. Based upon ^1H and ^{13}C NMR data, including labelling studies [33], this species is formulated as the *eight-membered,* metallacyclic complex $Ta(=NBu^t{=}CHBu^t{=}CHCBu^tHCH_2)(OAr)_2$ (**36**), shown in Scheme 15. Although **36** is formed in only small concentrations and cannot be isolated, an adduct of this species, $Ta(=NBu^t{=}CHBu^t{=}CHBu^tHCH_2)(OAr)_2 \cdot 2NCMe$ (**36**-NCMe) has been isolated by performing the decomposition of $[\eta^2(N,C)\text{-}2,4,6\text{-}NC_5Bu^t_3H_2]Ta(OAr)_2Me$ (**14**) in the presence of a coordinating ligand (excess PMe_3), followed by crystallization from acetonitrile/Et_2O solutions. The eight-membered metallacycle $Ta(=NBu^t{=}CHBu^t{=}CHBu^tHCH_2)(OAr)_2$ (**36**) can be considered as a "ring expansion" product arising from the seven-membered metallacycle **19**. An analogy between the classic "ring

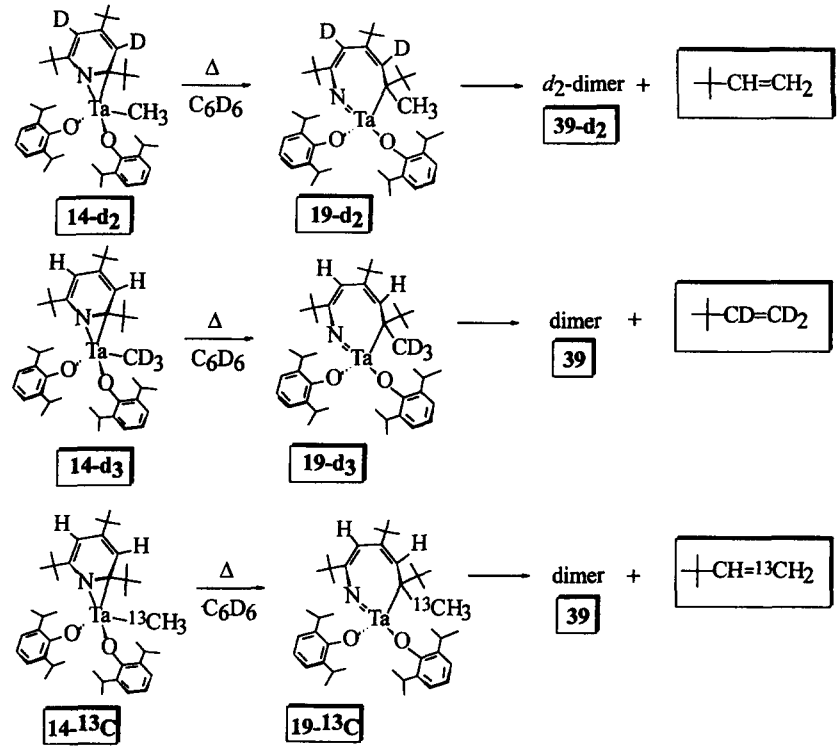

Scheme 16.

contraction" reaction, established in tantalacyclo*pentane* → tantalacyclo*butane* rearrangements [119,120] and our formal "ring expansion" process may be drawn to provide a reasonable mechanism of the **19** → **36** conversion. Therefore, we propose that a simple β-hydrogen elimination to provide transient $Ta(=NBu^t{-}CHBu^t{-}CHBu^t{-}CH_2)(H)(OAr)_2$ (**35**) occurs and that **35** subsequently undergoes rapid olefin reinsertion in the opposite sense to afford $\overline{Ta(=NBu^t{-}CHBu^t{-}CHBu^tHCH_2)}(OAr)_2$ (**36**), as shown in Scheme 17. This species can then afford a metallapyridine *monomer* by one of two possible routes: (1) Either **36** undergoes a six-electron, electrocyclic rearrangement to form the substituted bicyclic complex **37a** (Scheme 17), followed by a retro [2+2] cycloaddition of the metallacyclobutane portion of **37a** to provide the monomeric metallapyridine **38a** and $Bu^tCH{=}CH_2$; or (2) the **36** → **38b** + $Bu^tCH{=}CH_2$ conversion may be effected by a *β-alkyl elimination* [121,122], a process that would maintain the strong Ta=N multiple bond through intermediate **37b** and circumvent both putative intermediates **37a** and **38a**. Dimerization of **38** would afford the metallapyridine dimer $[\overline{Ta(\mu\text{-}NBu^t{-}CHBu^t{=}CH)}(OAr)_2]_2$ (**39**). Fortunately, we have recently isolated a monomeric metallapyridine (the THF adduct of **38**) that is described below.

The other C—N bond cleavage products $\overline{Ta(=NBu^t{-}CHBu^t{-}CHBu^tR)}(OAr)_2$ [R = Et (**20**), Pr^n (**21**), Bu^n (**22**)] also decomposes upon exhaustive thermolysis to form $[\overline{Ta(\mu\text{-}NBu^t{=}CHBu^t{=}CH)}(OAr)_2]_2$ (**39**) and the substituted *tert*-butylethylenes $Bu^tCH{=}CHR'$ as the only products. Thus, for $\overline{Ta(=NBu^t{=}CHBu^t{=}CHBu^tEt)}(OAr)_2$ (**20**), *cis*- and *trans*-$Bu^tCH{=}CHMe$ are identified; thermolysing $\overline{Ta(=NBu^t{=}CHBu^t{=}CHBu^tPr^n)}(OAr)_2$ (**21**), forms *cis*- and *trans*-$Bu^tCH{=}CHEt$; and for $\overline{Ta(=NBu^t{=}CHBu^t{=}CHBu^tBu^n)}(OAr)_2$ (**22**), *cis*- and *trans*-$Bu^tCH{=}CHPr^n$ are produced, Scheme 18. These results are consistent with the mechanism proposed in Scheme 17 for the ring degradation of $\overline{Ta(=NBu^t{=}CHBu^t{=}CHBu^tMe)}(OAr)_2$ (**19**) since these products constitute the *exact alkenes predicted by this mechanism* when **20**–**22** are decomposed. This analogous mechanism for **20**–**22** decomposition is shown in Scheme 18. This proposal is supported by the labeling experiments used to develop Scheme 17 and provides a clear explanation for how both *cis*- and *trans*-$Bu^tCH{=}CHR'$ arise. Since the complexes $\overline{Ta(=NBu^t{=}CHBu^t{=}CHBu^tR)}(OAr)_2$ (**20**–**22**) contain diasterotopic β-hydrogens and since one of these β-hydrogens must nearly eclipse the metal center to undergo β-hydrogen elimination (viewed down the C_α—C_β bond), then both possible olefin stereochemistries may be obtained, depending upon which β-hydrogen is eliminated, Scheme 18. The observed olefin stereochemistry in $Bu^tCH{=}CHR'$ is therefore set at the β-H elimination step and *prior* to subsequent reinsertion and ring expansion as indicated in Scheme 18 [33].

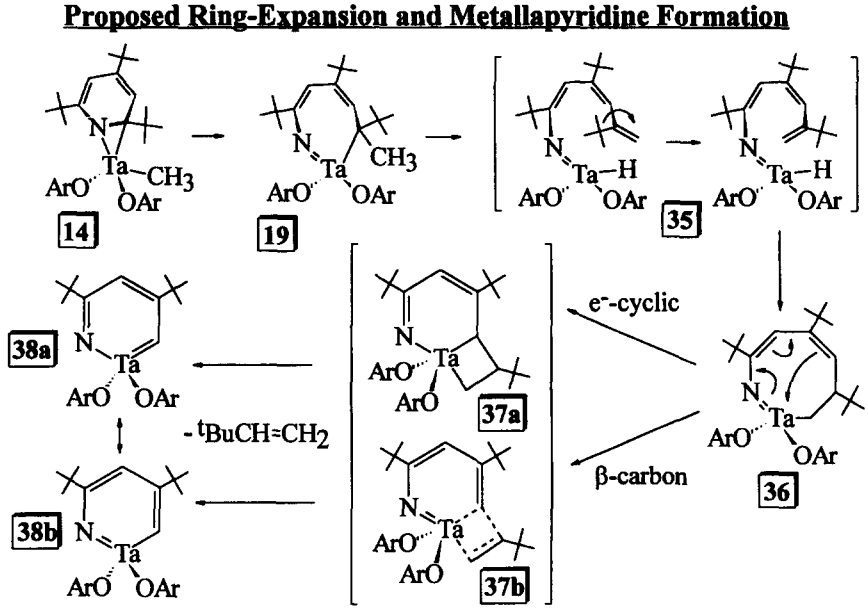

Scheme 17.

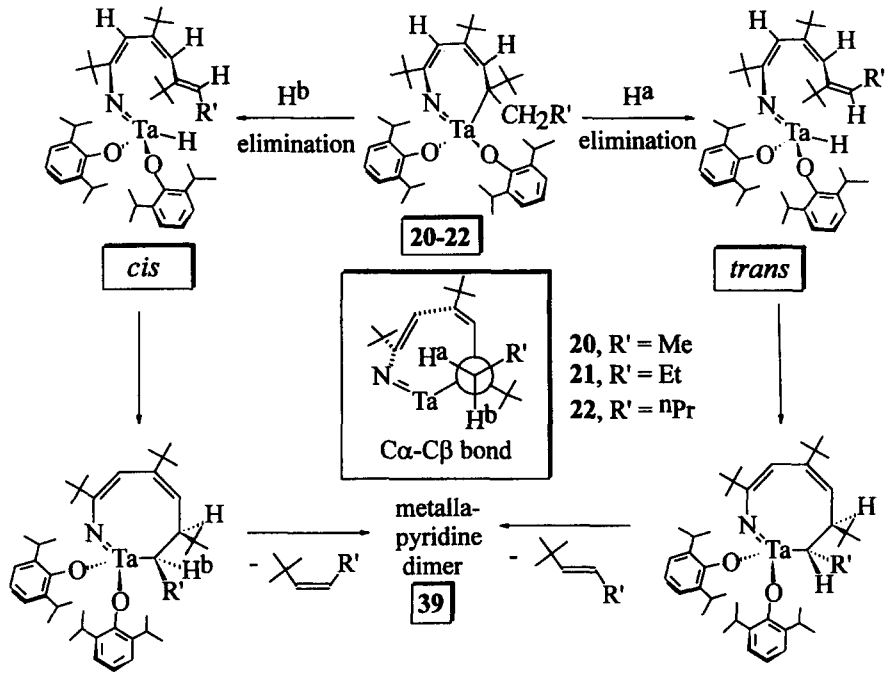

Scheme 18.

With the exception of **38,** all of the kinetic products in Scheme 15 have been observed *via* ^{1}H NMR and **12, 14, 19** and **39** have been *isolated* as the complexes shown, with **36** being isolated as its MeC≡N adduct [33]. Although it is logical that the metallapyridine dimer **39** is formed from the dimerization of **38,** which is sufficiently short-lived in solution that it is not observed, monomeric **38** has been an elusive species. However, thermolysing toluene solutions of $[\eta^2(N,C)$-2,4,6-$NC_5Bu^t_3H_2]Ta(OAr)_2Me$ (**14**) in the presence of THF affords a new species that has been identified as an adduct of **38** [35]. The ^{1}H NMR spectrum of this red complex reveals two sharp singlets at δ 7.41 and 5.97 for the metallacyclic protons (C_6D_6) and only *two* Bu^t resonances in its ^{1}H NMR spectrum, along with signals for a coordinated THF. Based upon its ^{1}H and ^{13}C NMR spectra, as well as its elemental analysis, this new complex is formulated as the

metallapyridine *monomer*, Ta(NCBu^{t}CHCBu^{t}CH)$(OAr)_2$(THF), **38**·THF.

There are two configurations for **38**·THF, both *Cs* symmetric, that are consistent with the ^1H and ^{13}C NMR data. Both structures **38**·THFa and **38**·THFb are trigonal bipyramids with the coordinated THF assuming an apical position and the aryloxide ligands occupying equatorial sites. The metallapyridine ring itself can be oriented such that the imido nitrogen is either *trans* to the THF ligand (as in **38**·THFa) or *cis* to the THF (as in **38**·THFb).

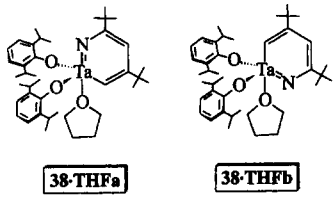

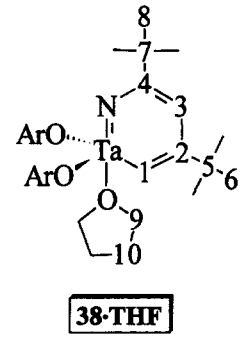

Fig. 6. Numbering scheme for the metallapyridine and THF carbon nuclei used in specifying ^1H and ^{13}C NMR assignments in Ta(=NCBu^t=CHCBu^t=CH)$(OAr)_2$(THF) (**38**·THF).

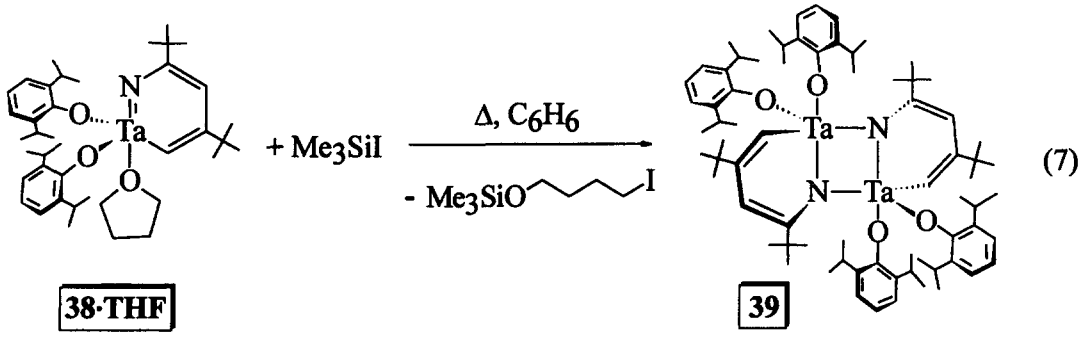

In order to determine which structure **38**·THF adopts in solution, as well as to make complete NMR assignments, a NOESY experiment was carried out. Two NOE cross peaks were observed between the resonance at δ 5.97 and both Bu^t groups (at δ 1.34 and 0.95), whereas only one cross peak was observed between the δ 7.41 proton and the Bu^t resonance at δ 1.34, thereby establishing the δ 5.97 and 7.41 resonances as C3*H* and C1*H*, respectively, Fig. 6. In addition, an NOE cross peak was observed between the THF Cα*H* resonance at δ 3.89 and C1*H*. Based upon these observations, the structure of **38**·THF can be assigned as that of **38**·THFa, with the Bu^t C6*H* and C8*H* resonances assigned at δ 1.34 and 0.95, respectively, Table 1. With the exception of C2, C4, C5 and C7, the ^{13}C NMR spectrum of **38**·THF is also completely assigned based upon these NOESY data and a HETCOR experiment. In the interest of making complete spectral assignments, a Heteronuclear Multiple Bond Correlation (HMBC) experiment was also carried out [123] and all the ring carbons can now be conclusively assigned, Table 1. Thus, C1 appears farthest downfield at δ 178.5, C2 and C4 appear at δ 172.5 and 167.8, respectively, and C3 occurs at δ 121.4 (C_6D_6) [35].

One significant question concerning the structure of **38**·THF is the extent to which the metallacycle is delocalized [124]. An X-ray crystallographic study confirms the proposed structure of **38**·THF as the metallapyridine monomer Ta(NCBu^{t}CHCBu^{t}CH)$(OAr)_2$(THF) [35]. The asymmetric unit contains two crystallographically independent, but virtually identical molecules; preliminary data for one molecule are shown in Fig. 7. Complex **38**·THF adopts a slightly distorted trigonal bipyramidal configuration with the aryloxide oxygens and metallacyclic C(1) occupying equatorial positions, in agreement with the solution structure; the THF ligand and metallacyclic nitrogen occupy axial positions. The $TaNC_4$ metallacycle is very nearly planar (mean deviation from planarity = 0.02 Å), but *it is not aromatic*, as discrete single and double bonds are evident around the ring, Fig. 7. This π-electron localization clearly favors the *imido* form shown (i.e. Ta(=NCBu^t=CHCBu^t=CH)$(OAr)_2$(THF)) rather than carbene structure, which is especially significant since the metal can dictate that either structure be adopted. Although the imido ligand in **38**·THF is strongly bent [Ta=N—C(4) = 148.0(8)°], it is only weakly basic as

Table 1. Summary of ^1H and ^{13}C NMR data for Ta(=NCBu^t=CHCBu^t=CH)(OAr)$_2$(THF) (**38**·THF)[a]

Assignment	^1H	^{13}C
C1H	7.41 (s)	178.51
C2		172.48
C3H	5.97 (S)	121.41
C4		167.84
C5		37.98
C6H	1.34 (s)	31.40
C7		36.58
C8H	0.97 (s)	28.96
C9H (CαH THF)	3.89 (mult)	71.62
C10H (CβH THF)	1.19 (mult)	25.42
C*H*Me$_2$	3.74 (spt)	27.25
CH*Me*$_2$	1.37 and 1.33 (d)	24.12, 23.99
H$_{aryl}$	7.22–6.96 (A$_2$B mult)	
C$_{ipso}$		160.05
C$_o$		136.73
C$_m$		123.29
C$_p$		121.58

[a] C_6D_6 at probe temperature.

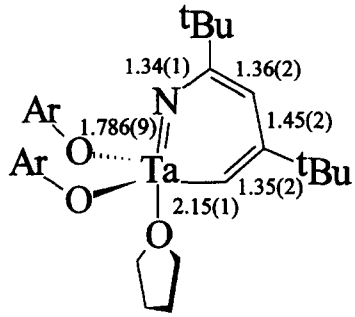

Fig. 7. Selected metallapyridine bond lengths (Å) for molecule A of Ta(=NCBu^t=CHCBu^t=CH)(OAr)$_2$(THF) (**38**·THF).

attempts to alkylate the imido nitrogen with electrophiles (e.g. MeI) were unsuccessful.

Although base-free **38** is not observed by ^1H NMR spectroscopy during the thermal conversion of **14** to dimer **39**, its intermediacy is supported by the fact that Ta(=NCBu^t=CHCBu^t=CH)(OAr)$_2$(THF) (**38**·THF) can be cleanly converted into **39**. Despite the fact that the THF ligand in **38**·THF appears to be labile (e.g. the THF is easily displaced by pyridine), heating solutions of **38**·THF does not lead to the formation of **39**. However, heating a cherry red solution of **38**·THF with Me_3SiI results in the decolorization of the solution and the formation of insoluble red crystals, eq. (7) [35]. The only product observable in solution by ^1H NMR is Me_3Si $OCH_2CH_2CH_2CH_2I$, which arises from ring cleavage of the THF of **38**·THF [125]. The insoluble red crystals were identified as dimer **39** by elemental analysis and by comparison of one crystal's unit cell parameters to those of an authentic sample of **39** [33].

These observations complete the reaction sequence in Scheme 15, delineate one process by which heterocyclic C—N bonds are cleaved and offer new insight into how nitrogen heterocycles may be further degraded *after* C—N bond cleavage. Information on subsequent heterocycle degradation reactions may be relevant to catalytic HDN since under normal HDN conditions ethane, ethylene, propane and propylene are the principal products of pyridine HDN with only a *minor fraction* of C_5 products being generated [16].

5. *New models for* C—N *cleavage in quinoline hydrodenitrogenation*

We have also explored a series of C—N *bond-forming* reactions that have afforded a striking suggestion for how quinoline may undergo denitrogenation in its conversion to indene, as Fish has observed [126]. These reactions are based upon attempts to generate dihydropyridine complexes through the 4+2 cycloaddition of butadienes and nitriles [127]. The unexpected, net 4+1 addition of N≡CR to the diene ligand in (η^4-diene)Ta(OAr)$_3$ complexes, in conjunction with the nucleophile-induced C—N scission reactions described above, constitute a new model for quinoline hydrodenitrogenation [128].

The reaction of Ta(OAr)$_3$Cl$_2$(OEt$_2$) with Mg(C_4H_6)(dme) (dme = 1,2-dimethoxyethane) affords yellow crystals of the butadiene adduct Ta(η^4-C_4H_6)(OAr)$_3$ (**40**) shown in Scheme 19. Yellow crystals of the η^4-isoprene complex Ta(η^4-2-MeC_4H_5)(OAr)$_3$ (**41**) are isolated from the NaHg reduction of Ta(OAr)$_3$Cl$_2$(OEt$_2$) in the presence of isoprene. Scheme 19. Although excess isoprene is employed to drive the synthesis of **41** to completion, there is no indication that insertion of a second equivalent of the diene into the tantalum–carbon bonds of Ta(η^4-2-MeC_4H_5)(OAr)$_3$ (**41**) occurs under these conditions, in contrast to butadiene complexes of zirconium [129]. We assume the η^4-diene ligands in **40** and **41** are highly reduced and therefore structurally similar to Rothwell's Nb(OC_6H_3Ph-η^4-C_6H_7)(O-2,6-$C_6H_3Ph_2$)$_2$ [130].

If the reaction between Ta(η^4-2-MeC_4H_5)(OAr)$_3$ (**41**) with 1 equiv. of N≡CMe (in pentane) is worked up *immediately* after mixing these reagents, the metallacycloimine product Ta(N=CMeCH$_2$CMe=CHCH$_2$)(OAr)$_3$ (**42**) can be isolated, Scheme 19. Upon reacting Ta(η^4-2-MeC_4H_5)(OAr)$_3$ (**41**) with pivalonitrile or benzonitrile N≡CR (R = Bu^t or Ph, respectively) in pentane, the analogous metallacyclic insertion products Ta(N=CRCH$_2$CMe=CHCH$_2$)(OAr)$_3$ **43** (R = Bu^t) and **44** (R = Ph) are also formed in high yield, Scheme 19. (We draw these as η^1-allylic, but note that η^3-allylic metallacycles are possible [131].) Both ^1H and ^{13}C NMR spectroscopy indicate that a single regioisomer is formed in these reactions

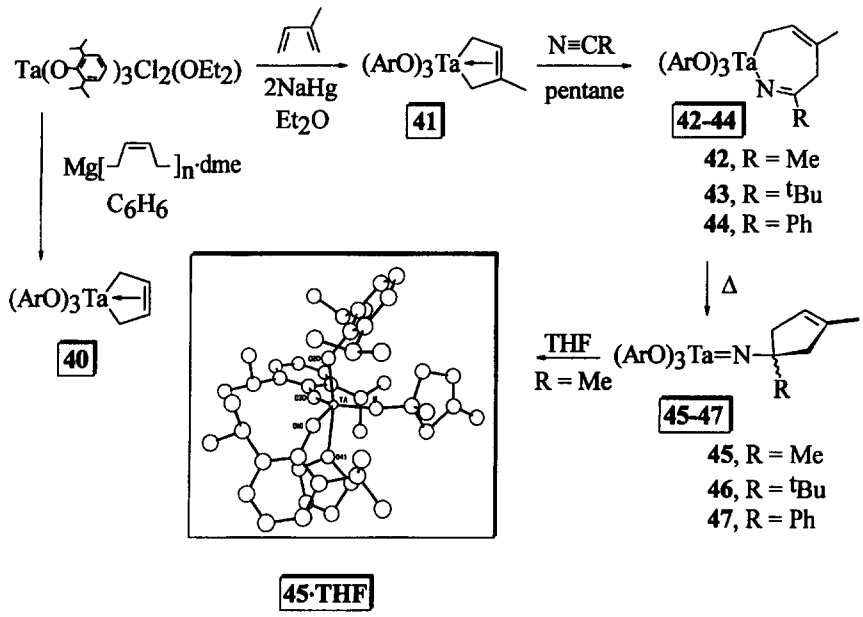

Scheme 19.

and the isomers presented in Scheme 19 were confirmed by HETCOR experiments. However, these complexes were discovered to be kinetic products of the reactions: after several hours, the reaction between Ta(η^4-2-MeC_4H_5)$(OAr)_3$ (**41**) and N≡CMe affords a new product **45** that we formulate as the *cyclopentenylimido* complex Ta(=NCMeCH_2CMe=CHCH_2)$(OAr)_3$, indicated in Scheme 19. Ta(N=CMeCH_2CMe=CHCH_2)$(OAr)_3$ (**42**) is confirmed as an intermediate in the **41** → **45** conversion, since isolated **42** undergoes the smooth, room-temperature conversion to Ta(=NCMeCH_2CMeCHCH_2)$(OAr)_3$ (**45**). The pivalonitrile and benzonitrile insertion products **43** and **44** are stable as the metallacycloimines at room temperature, however, heating solutions of these compounds ($\geqslant 80°C$) induces a rearrangement and the corresponding cyclopentenyl imido complexes **46** and **47** are isolated, Scheme 19. The mechanism(s) and synthetic utility of these reactions are under investigation, but one may envision a simple electrocyclic rearrangement, driven by formation of the strong metal–nitrogen multiple bond.

Our formulation of **45** as the cyclopentyl imido complex Ta(=NCMeCH_2CMe=CHCH_2)$(OAr)_3$ was achieved by NMR spectroscopy and a preliminary X-ray crystallographic study. Ta(=NCMeCH_2CMe=CHCH_2)$(OAr)_3$ (**45**) was difficult to crystallize, except in the presence of THF, in which case the adduct **45**·THF formed as moderate to poor quality crystals. The preliminary structure of **45**·THF establishes its overall trigonal bipyramidal geometry, an equatorial nitrogen ligand, clear unsaturation of the carbocycle as shown in Scheme 19, an N—C single bond [1.43(4) Å], and the Ta=N multiple bond of 1.84(2) Å, indicative of an imido linkage. We believe that the same driving force that allowed the C—N bond cleavage reactions described earlier to proceed, namely the formation of Ta—N multiple bond, as well as the energy gained in *forming* new N—C bonds, contribute to the formation of **45**–**47**. Previous examples of 4+1 reactions have been described by Eaton [132–134], and by Erker [135], but none involving nitriles.

In addition to its potential synthetic utility, the rearrangement in Scheme 19 may be relevant to some interesting observations by Fish and coworkers concerning quinoline HDN over a $Ni/SiO_2/Al_2O_3$ catalyst [126]. In addition to the formation of propyl benzene and propyl cyclohexane in this reaction, both indene and indan are formed in smaller amounts, Scheme 20. If we juxtapose the C—N bond scissions in Schemes 7 and 11 with the **42** → **45** rearrangement described here, we can suggest a simple reactivity model that accounts for these observations. Scheme 21 suggests how indene could arise from quinoline coordination [30,31], C—N bond scission [33] and ring rearrange-

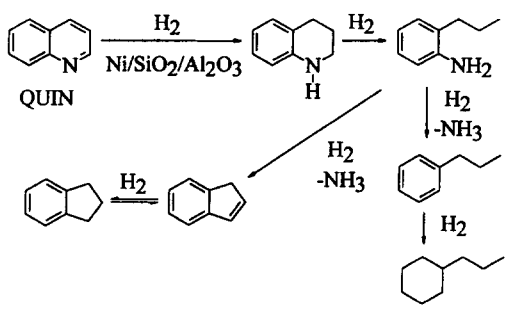

Scheme 20.

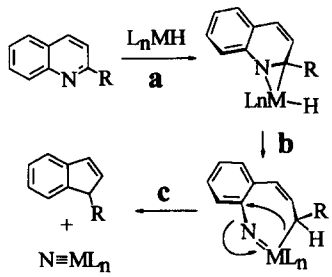

Scheme 21.

ment [128], based upon reactivity precedent in aryloxide supported tantalum complexes. Thus, step c of Scheme 21 may be compared to the rearrangements outlined in Scheme 19 above. We have observed an *imine* nitrogen being converted to an *imido* nitrogen (Scheme 19), while step c (Scheme 21) suggests a metallacycle *imido* ligand being converted into a *nitrido* ligand.

6. *Tetrahydroquinolinyl and indolinyl complexes as models for substrate–catalyst adducts in hydrodenitrogenation catalysis*

A generalized HDN reaction scheme for quinoline was presented in Scheme 1. Regardless of which pathway is ultimately productive, the most facile step of quinoline HDN is hydrogenation of the heterocycle, therefore, quinoline HDN involves the intermediacy of tetrahydroquinoline, just as the indole HDN reaction pathway includes indoline. While there are several reports of quinoline complexes [30,56–58] and catalytic HDN studies invariably examine quinoline and indole substrates [29,87,89,113,136–138] complexes of their hydrogenated derivatives tetrahydroquinoline or indoline are scarce [29,139,140]. Accordingly, we have prepared complexes containing the *amido* ligands of tetrahydroquinoline, namely tetrahydroquinolinyl $[NC_9H_{10}]^-$. These compounds were deemed worthy synthetic targets, since they more closely resemble the substrate–catalyst complexes at the active site in HDN as compared to simple quinoline adducts. Additionally, because the $\eta^2(N,C)$ binding mode provides excellent reactivity models for fundamental HDN reactions of pyridines, we wanted to determine whether η^1 complexes of tetrahydroquinoline, or of its amide, might serve as precursors to related η^2 species. Such complexes would model Laine's mechanistic proposal for pyridine/piperidine HDN that includes an $\eta^2(N,C)$-piperidyl ligand, Scheme 2 [7,8].

The reactions of $TaCl_5$ with $Me_3SiNC_9H_{10}$ or $LiNC_9H_{10}$, where NC_9H_{10} = tetrahydroquinolinyl, afford selective preparative routes to the complete series of amido halide complexes of tantalum(V) **48–52** as shown in Scheme 22. Thus, the mono (tetrahydroquinolyl) complex is isolated as an ether adduct $Ta(NC_9H_{10})Cl_4(OEt_2)$, while the complexes $Ta(NC_9H_{10})_nCl_{5-n}$ (n = 2–5) are found to be base-free, monomeric species. An X-ray structural determination of $Ta(NC_9H_{10})_2Cl_3$ (**49**) reveals that it adopts a trigonal bipyramidal geometry with equatorial amido ligands that are closer to lying parallel (within) rather than perpendicular to the equatorial plane of the trigonal bipyramid, Fig. 8.

We also sought aryloxide-supported $\eta^1(N)$-NC_9H_{10} compounds of the form $Ta(NC_9H_{10})_x(OAr)_yR_z$ for the prospect of cyclometallating a NC_9H_{10} ligand to afford $\eta^2(N,C)$-heterocyclic species. Thus, $Ta(NC_9H_{10})(OAr)Cl_3(OEt_2)$ (**53**), $Ta(NC_9H_{10})_2(OAr)_2Cl$ (**54**) and their alkyl derivatives were prepared as indicated in Scheme 23. The alkyl derivatives $Ta(NC_9H_{10})(OAr)Me_2Cl$ (**55**), $Ta(NC_9H_{10})(OAr)Et_2Cl$ (**56**) and $Ta(NC_9H_{10})_2(OAr)_2Me$ (**57**), as well as the amido derivatives $Ta(NC_9H_{10})_4Cl$ (**51**), $Ta(NC_9H_{10})_5$ (**52**) and $Ta(NC_9H_{10})Me_2Cl_2$ (**58**) (prepared from **48** and $ZnMe_2$) were all thermolysed in an attempt to cyclometallate a NC_9H_{10} ligand and eliminate alkane or HNC_9H_{10}, much in the way that $Ta(NEt_2)_5$ undergoes thermolysis to form the *N*-ethylethyleneimine complex $Ta(\eta^2\text{-EtN=CHCH}_3)(NEt_2)_3$, Scheme 24 [141–144]. Unfortunately, thermolysing **56–58** in C_6D_6 solution (80°C, up to 24 h) afforded no evidence for the formation of any $\eta^2(N,C)$-heterocycles; intractable mixtures that included paramagnetic species were slowly formed. While thermolysis of $Ta(NC_9H_{10})_4Cl$ (**51**) and $Ta(NC_9H_{10})_5$ (**52**) under similar conditions (C_6D_6, $\geqslant$80°C) produced free tetrahydroquinoline HNC_9H_{10}, no evidence for the formation of an $\eta^2(N,C)$ complex was obtained in either case; intractable, paramagnetic products were again obtained.

In order to test whether a *reversible* metallation of a NC_9H_{10} ligand occurs under these conditions [27,73], a sample of $Ta(NC_9H_{10})_5$ (**52**) was thermolysed in the presence of excess DNC_9H_{10} and examined by ^1H and ^{13}C NMR [145]. No incorporation of deuterium into either H2 or H8 (or any position) of the coordinated NC_9H_{10} amide ligand was observed. We note that Gambarotta recently described the preparation of $Nb[\eta^2(N,C)\text{-CyN=C}_6N_{10}](NCy_2)_2Cl$ (Cy = C_6H_{11}) from $NbCl_4(THF)_2$ and $LiNCy_2$, containing one metallated cyclohexyl ring [146]. The proposal is made that intermediate $Nb(NCy_2)_3Cl$ is formed that undergoes a formal elimination of hydrogen, therefore, under the appropriate conditions these cyclometallations are facile [146]. Gambarotta has also described the tantalum analog $Ta[\eta^2(N,C)\text{-CyN=C}_6H_{10}](NCy_2)_2Cl$ from $TaCl_5$ and $LiNCy_2$ that could form by $HNCy_2$ elimination from intermediate $Ta(NCy_2)_4Cl$ [147]. These reactions are perhaps facilitated by the greater steric congestion of the NCy_2 amides relative to NC_9H_{10}, as well as possible one electron pathways that are operative in the niobium system.

7. *Significance of recent model studies*

Despite its importance in producing high-quality, low-cost fuels and feedstocks, HDN catalysis is sig-

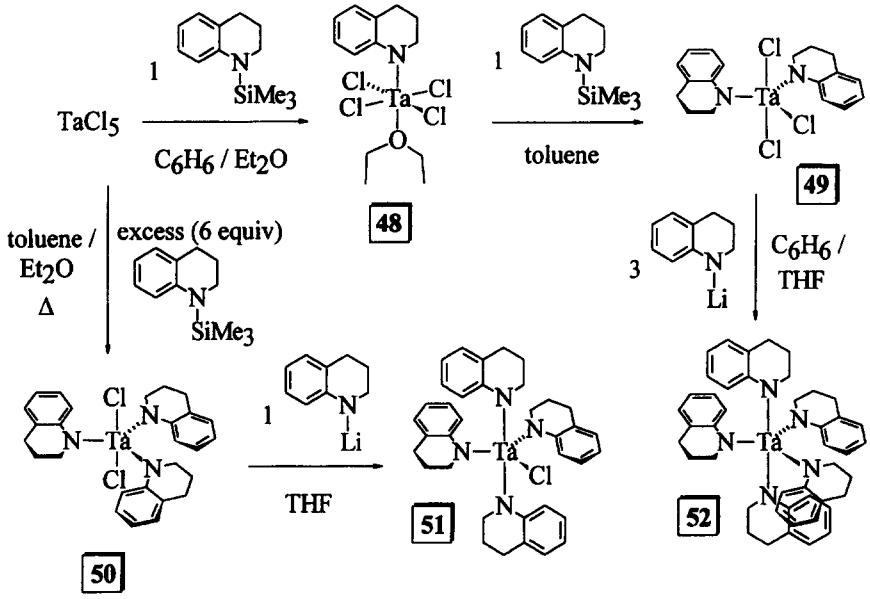

Scheme 22.

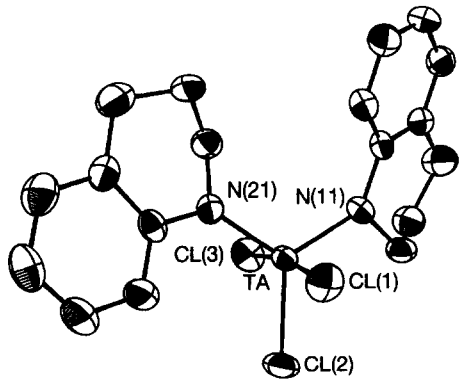

Fig. 8. Molecular structure of $Ta(NC_9H_{10})_2Cl_3$ (**49**), Ta—N(11) = 1.932(5), Ta—N(21) = 1.932(5) Å, N(11)—Ta—N(21) = 116.8(2)°, Cl(1)—Ta—Cl(3) = 170.27(7)°.

nificantly less well-studied than HDS. In particular, the C—N bond scission step has been elusive since discrete C—N cleavage reactions that were amenable to study were rare. Therefore, an examination of our model reactions in view of proposed methods of C—N cleavage is instructive and may allow us to draw some conclusions regarding ways in which heterocyclic C—N bonds may be cleaved.

Scheme 2 summarizes Laine's proposal for C—N bond scission in piperidine [7]. A crucial feature of this proposal is the existence of an $\eta^2(N,C)$ piperidine *amido* complex that is formed in a C—H activation step at the catalytic site. The subsequent C—N bond cleavage step involves hydride attack at either Cα, with the formation of an intermediate amido complex, or attack at N, with the formation of an alkylidene. The C—N bond cleavage step we have observed with carbon nucleophiles (Scheme 11) shares three similarities with Laine's proposal. First, cleavage is found to occur only in an $\eta^2(N,C)$ complex. We have also demonstrated that the $\eta^2(N,C)$ bonding mode in complexes of quinoline permits facile hydrogenation of the heterocycle (without reducing the carbocycle) and that $\eta^1(N)$ quinoline complexes are not readily reduced [30]. In this system, C—N bond scission has not been induced in d^0 or d^1 $\eta^1(N)$-pyridine or $\eta^1(N)$-quinoline complexes. Wolczanski's C—N scission in pyridine also occurs only in an $\eta^2(N,C)$ complex [36]. Secondly, we have demonstrated that in the $\eta^2(N,C)$ mode, attack occurs at the pyridine *carbon*, rather than the nitrogen. In the metallaaziridine description of the $\eta^2(N,C)$-pyridine, this reaction in our complexes transforms a formal *amido* nitrogen in the η^2-pyridine to a formal *imido* nitrogen in the ring-opened structure in a reaction driven largely by the formation of a strong metal–ligand multiple bond. Laine's proposal differs from our observation in that under actual HDN conditions, the heterocyclic ring will be hydrogenated such that a formal *amine* nitrogen in the η^2-piperidyl ligand is converted to an *amido* nitrogen upon C—N bond cleavage. Thirdly, C—N bond scission occurs *via* an *intra*molecular, *endo* attack of the migrating ligand. The results obtained for the carbon nucleophiles may also reflect the mechanism of C—N scission by hydride, since metal-mediated hydride attack on $\eta^2(N,C)$-heterocycles now appears to be a reasonable pathway.

Finally, our model system also offers insight into how nitrogen heterocycles may be further degraded *after* C—N *bond cleavage* in HDN catalysis. An $\eta^2(N,C)$-pyridine ligand that ring opens in a manner so as to generate β hydrogens may be subject to further

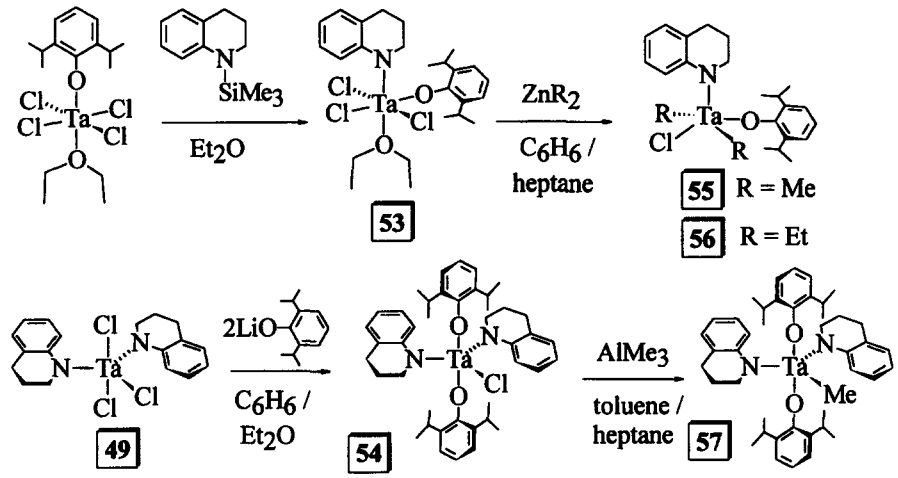

Scheme 23.

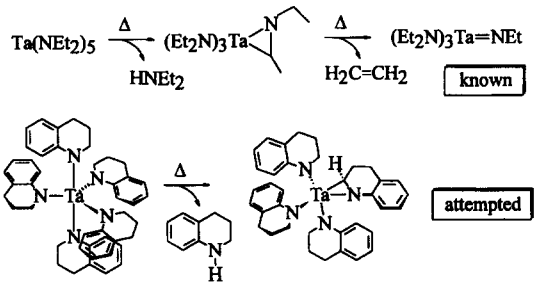

Scheme 24.

degradation, since pathways exist for C—C bond cleavage by rearrangement of the ring-opened complex. Such information may be relevant to catalytic HDN since under normal HDN conditions ethane, ethene, propane and propene are the principal products of pyridine HDN with only a minor fraction of C_5 products being generated [16].

Our observations are also consistent with the heterogeneous studies of Perot and coworkers [85,113]. The Perot experiment (Scheme 4) revealed that under the same conditions that quinoline reacts to give primarily THQ, tetrahydroisoquinoline undergoes HDN to afford primarily 2-ethyltoluene, consistent with an SN mechanism of C—N bond cleavage in this compound. Perot notes that substitutions at the carbon α to nitrogen result in changes in the HDN product distribution, perhaps signalling a change in mechanism for the C—N scission step [85].

The overall reaction we have observed between the pyridine complex $[\eta^2(N,C)$-2,4,6-$NC_5Bu^t_3H_2]Ta(OAr)_2Cl$ and an attacking carbon nucleophile (Schemes 10–14) can be partitioned into two stages: (1) nucleophilic attack at the metal center, followed by (2) nucleophilic migration to the η^2 ligand. In our model system, this migration is the rate-limiting step. The role of the metal center therefore is to mediate this process: it selectively activates the heterocyclic C—N bond and renders the pyridine Cα susceptible to nucleophilic attack. This nucleophilic designation is based upon a very slight rate enhancement in aryl migration using electron-donating substituents in the *para* position of the aryl ring. Nevertheless, the data from our model system are consistent with both nucleophilic attack of the migrating ligand on the pyridine Cα and with Perot's evidence for SN mechanisms in tetrahydroisoquinoline HDN.

Finally, these observations may constitute a framework on which to unify the Laine and Perot theories of C—N scission in the following ways. As Laine suggests, substrate coordination is required and we have found that $\eta^2(N,C)$ is the most relevant bonding mode since C—N bond cleavage has been observed in heterocycles bound in this mode only. Furthermore, an *intra*molecular migration of the attacking nucleophile achieves C—N scission. Bonding the pyridine $\eta^2(N,C)$ allows the pyridine Cα (a formal sp^2 carbon) to attain sp^3 hybridization and thereby renders this carbon subject to nucleophilic attack. If one considers the $\eta^2(N,C)$ piperidyl amine complex (**3a** ↔ **3b**) that is proposed by Laine, it is clear that the Lewis acidic, electrophilic metal center can take the place of H^+ in the classic nucleophilic substitution mechanism of Scheme 2, as indicated by structure **3b**. In this way, nucleophilic displacement of the C—N bonding electrons cleaves this bond while the N–metal bond is maintained, therefore, $\eta^2(N,C)$ binding serves the same purpose as protonation of the substrate nitrogen.

SUMMARY AND CONCLUSIONS

The results described in this report allow the following conclusions to be drawn and suggest the extent to which this system constitutes a valid reactivity model for the active site in HDN catalysts.

(1) These studies have demonstrated the $\eta^2(N,C)$ coordination mode of relevant HDN substrates such as substituted pyridines and quinolines and established a correlation between oxidation state and preferred bonding mode. We have also uncovered an $\eta^1(N) \rightarrow \eta^2(N,C)$ rearrangement in quinoline upon reduction of its complexes from d^0 to d^2.

(2) Structural and reactivity evidence from our studies and from those of Wolczanski [48] point to a disruption of aromaticity of the heterocycle in $\eta^2(N,C)$-pyridine compounds. Since the $\eta^2(C,C)$-pyridine or $\eta^2(C,C)$-quinoline coordination modes have not been observed in d^2 tantalum complexes, this interruption of aromaticity accompanies a selective activation of the heterocycle's C—N bond.

(3) Carbon–nitrogen bond cleavage is found to occur only in the $\eta^2(N,C)$-pyridine complexes and therefore only in the d^2 oxidation state. Given that the cobalt–promoter effect in MoS_2/γ-Al_2O_3 may include an electron transfer role [12], our observations are perhaps relevant to changes in the substrate binding mode at the active site.

(4) The $\eta^2(N,C)$ binding mode renders an HDN substrate susceptible to nucleophilic attack. The overall reaction can be partitioned into two stages: nucleophilic attack at the metal center followed by ligand migration to the η^2 ligand. In our model system, this migration is rate-limiting.

(5) Nucleophilic attack on an $\eta^2(N,C)$-pyridine ligand occurs invariably at the pyridine *carbon*, rather than nitrogen, to form a metallacyclic imido complex, consistent with Laine's proposal. Therefore, C—N bond scission appears to be driven by, in large part, the formation of a strong metal–nitrogen multiple bond, as well as the reduction in the pyridine C—N bond order that arises from its $\eta^2(N,C)$ coordination. Since imido ligands are apparently involved in other catalytic processes where the nitrogen is ultimately removed from the metal (e.g. propylene ammoxidation [148–153] and nitrile reduction [154–156]), the fact that the ring-opening reaction occurs with the formation of an imido ligand M=NR is consistent with the ultimate elimination of ammonia from the catalyst site.

(6) The C—N bond scissions observed in these complexes occur unambiguously *via* an *intra*molecular, *endo*-attack of the attacking ligand that migrates to the HDN substrate as a σ *nucleophile*. Therefore, the same metal center in this model system is capable of activating the pyridine C—N bond and delivering the reagent (alkyl and perhaps hydride) that induces C—N bond scission.

(7) While there is no evidence that the Co–Mo–S or Ni–Mo–S phases in cobalt- or nickel-promoted MoS_2/γ-Al_2O_3 can induce C—N scission *prior* to heterocycle hydrogenation [3], the reactions uncovered in this study offer the possibility that C—N bond cleavage may be promoted under milder conditions than are currently necessary. The possibility of reducing the consumption of H_2 by C—N scission *prior* to hydrogenation is not likely under existing hydrotreating conditions, since heterocycle hydrogenation (e.g. pyridine → piperidine or quinoline → 1,2,3,4-tetrahydroquinoline) is the most facile step in hydrotreating.

(8) Carbon–carbon bond scissions of a ring-opened complex appear to be possible at the same metal site. Thus, in cases where a highly substituted metallacycle arises from pyridine ring-opening, further degradation pathways for C—C bond cleavage exist.

Acknowledgments—We thank the Division of Chemical Sciences, Office of Basic Energy Sciences, Office of Energy Research, U.S. Department of Energy (DE-FG03-93ER14349) for support of this research. We also thank Mr Igor Filippov for his invaluable experimental assistance in the NMR studies. Dr David P. Smith (Affymetrix), Mr Kevin D. Allen (Shell Development Company) and Mr Richard P. Kingsborough (Massachusetts Institute of Technology) are due our thanks for their early work on the $\eta^2(N,C)$-quinoline complexes described in this contribution.

REFERENCES

1. Gary, J. H. and Handwerk, G. E., *Petroleum Refining: Technology and Economics*, 3rd edn. Marcel Dekker, New York, 1993.
2. Satterfield, C. N., *Heterogeneous Catalysis in Industrial Practice*, 2nd edn. McGraw-Hill, New York, 1991.
3. Angelici, R. J., in *Encyclopedia of Inorganic Chemistry*, Vol. 3, ed. R. B. King, John Wiley and Sons, New York, 1994, pp. 1433–1443.
4. Kasztelan, S., des Courières, T. and Breysse, M., *Catal. Today*, 1991, **10,** 433.
5. Ho, T. C., *Catal. Rev.-Sci. Engng.*, 1988, **30,** 117.
6. Ledoux, M. J., In *Catalysis*, Vol. 7, The Chemical Society, London, 1985, pp. 125–148.
7. Laine, R. M., *Catal. Rev.-Sci. Engng.*, 1983, **25,** 459.
8. Laine, R. M., *Ann. NY Acad. Sci.*, 1983, **415,** 271.
9. Fish, R. H., *Ann. NY Acad. Sci.*, 1983, **415,** 292.
10. Katzer, J. R. and Sivasubramanian, R., *Catal. Rev.-Sci. Engng.*, 1979, **20,** 155.
11. Prins, R., de Beer, V. H. J. and Somorjai, G. A., *Catal. Rev.-Sci. Engng.*, 1989, **31,** 1.
12. Harris, S. and Chianelli, R. R., *J. Catal.*, 1986, **98,** 17.
13. Danot, M., Afonso, J., Portefaix, J. L., Breysse, M. and des Courières, T., *Catal. Today*, 1991, **10,** 629.
14. Harvey, T. G. and Matheson, T. W., *J. Catal.*, 1986, **101,** 253.
15. De Los Reyes, J. A., Vrinat, M., Geantet, C. and Breysse, M., *Catal. Today*, 1991, **10,** 645.
16. Choi, J.-G., Brenner, J. R., Colling, C. W., Demczyk, B. G., Dunning, J. L. and Thompson, L. T., *Catal. Today*, 1992, **15,** 201.
17. Hamon, D., Vrinat, M., Breysse, M., Durand, B., Jebrouni, M., Roubin, M., Magnoux, P. and des Courières, T., *Catal. Today*, 1991, **10,** 613.
18. Breysse, M., Portefaix, J. L. and Vrinar, M., *Catal. Today*, 1991, **10,** 489.
19. Pecoraro, T. A. and Chianelli, R. R., *J. Catal.*, 1981, **67,** 430.
20. Chianelli, R. R., *Catal. Rev.* 1984, **26,** 361.

21. Fish, R. H., Thormodsen, A. D., Moore, A. D., Perry, D. L. and Heinemann, H., *J. Catal.*, 1986, **102,** 270.
22. Satterfield, C. N., Modell, M. and Wilkers, J. A., *Ind. Engng. Chem. Process Des. Dev.*, 1980, **19,** 154.
23. Satterfield, C. N. and Yang, S. H., *Ind. Engng. Chem. Process Des. Dev.*, 1984, **23,** 11.
24. Fish, R. H., Tan, J. L. and Thormodsen, A. D., *Organometallics*, 1985, **4,** 1743.
25. Fish, R. H., Tan, J. L. and Thormodsen, A. D., *J. Org. Chem.*, 1984, **49,** 4500.
26. Fish, R. H. and Thormodsen, A. D., *J. Am. Chem. Soc.*, 1982, **104,** 5234.
27. Fish, R. H., Baralt, E. and Smith, S. J., *Organometallics*, 1991, **10,** 54.
28. Jardine, I. and Mcquillin, F. J., *J. Chem. Soc. D*, 1970, 626.
29. Baralt, E., Smith, S. J., Hurwitz, J., Horváth, I. T. and Fish, R. H., *J. Am. Chem. Soc.*, 1992, **114,** 5187.
30. Allen, K. D., Bruck, M. A., Gray, S. D., Kingsborough, R. P., Smith, D. P., Weller, K. J. and Wigley, D. E., *Polyhedron*, 1995, **14,** 3315.
31. Gray, S. D., Smith, D. P., Bruck, M. A. and Wigley, D. E., *J. Am. Chem. Soc.* 1992, **114,** 5462.
32. Gray, S. D., Fox, P. A., Kingsborough, R. P., Bruck, M. A. and Wigley, D. E., *Am. Chem. Soc., Div. Pet. Chem. Prepr.*, 1993, **39,** 706.
33. Gray, S. D., Weller, K. J., Bruck, M. A., Briggs, P. M. and Wigley, D. E., *J. Am. Chem. Soc.*, 1995, **117,** 10678.
34. Weller, K. J., Gray, S. D., Briggs, P. M. and Wigley, D. E., *Organometallics*, 1995, **14,** 5588.
35. Weller, K. J., Filippov, I., Briggs, P. M. and Wigley, D. E., *J. Organomet. Chem.*, 1997, in press.
36. Kleckley, T. S., Bennett, J. L., Wolczanski, P. T. and Lobkovsky, E. B., *J. Am. Chem. Soc.*, 1997, **119,** 247.
37. Bonanno, J. B., Henry, T. P., Neithamer, D. R., Wolczanski, P. T. and Lobkovsky, E. B., *J. Am. Chem. Soc.*, 1996, **118,** 5132.
38. Tomasik, P. and Ratajewicz, Z., *Chem. Heterocycl. Compd. (Engl. Trans.)*, 1985, **14**(6), 1.
39. Reedijk, J., in *Comprehensive Coordination Chemistry*, Vol. 2, ed. G. Wilkinson, R. D. Gillard and J. McCleverty. Pergamon Press, Oxford, 1987, p. 73.
40. Davies, S. G. and Shipton, M. R., *J. Chem. Soc., Chem. Commun.*, 1989, 995.
41. Morris, R. H. and Ressner, J. M., *J. Chem. Soc., Chem. Commun.*, 1983, 909.
42. Timms, P. L., *Angew. Chem., Int. Ed. Engl.*, 1975, **14,** 273.
43. Simons, L. H., Riley, P. E., Davis, R. E. and Lagowski, J. J., *J. Am. Chem. Soc.*, 1976, **98,** 1044.
44. Wucherer, E. J. and Muetterties, E. L., *Organometallics*, 1987, **6,** 1691.
45. Wucherer, E. J. and Muetterties, E. L., *Organometallics*, 1987, **6,** 1696.
46. Pannell, K. J., Kalsotra, B. L. and Párkányi, C., *J. Heterocycl. Chem.*, 1978, **15,** 1057.
47. Neithamer, D. R., Párkányi, L., Mitchell, J. F. and Wolczanski, P. T., *J. Am. Chem. Soc.*, 1988, **110,** 4421.
48. Covert, K. J., Neithamer, D. R., Zonnevylle, M. C., LaPointe, R. E., Schaller, C. P. and Wolczanski, P. T., *Inorg. Chem.*, 1991, **30,** 2494.
49. Wolczanski, P. T., *Polyhedron*, 1995, **14,** 3335.
50. Strickler, J. R., Bruck, M. A. and Wigley, D. E., *J. Am. Chem. Soc.*, 1990, **112,** 2814.
51. Smith, D. P., Strickler, J. R., Gray, S. D., Bruck, M. A., Holmes, R. S. and Wigley, D. E., *Organometallics*, 1992, **11,** 1275.
52. Cordone, R. and Taube, H., *J. Am. Chem. Soc.*, 1987, **109,** 8101.
53. For related η^2-pyridinium complexes, see: Cordone, R., Harman, W. D. and Taube, H., *J. Am. Chem. Soc.*, 1989, **111,** 2896.
54. Drew, M. G. B., Mitchell, P. C. H. and Reed, A. R., *J. Chem. Soc., Chem. Commun.*, 1982, 238.
55. Drew, M. G. B., Baricelli, P. J., Mitchell, P. C. H. and Read, A. R., *J. Chem. Soc., Dalton Trans.*, 1983, 649.
56. Fish, R. H., Kim, H.-S. and Fong, R. H., *Organometallics*, 1989, **8,** 1375.
57. Fish, R. H., Kim, H.-S., Babin, J. E. and Adams, R. D., *Organometallics*, 1988, **7,** 2250.
58. Fish, R. H., Kim, H.-S. and Fong, R. J., *Organometallics*, 1991, **10,** 770.
59. Kerschner, D. L., Rheingold, A. L. and Basolo, F., *Organometallics*, 1987, **6,** 196.
60. Kvietok, F. A., Allured, V., Carperos, V. and Rakowski Dubois, M., *Organometallics*, 1994, **13,** 60, and refs therein.
61. Kuhn, N., *Bull. Soc. Chem. Belg.*, 1990, **99,** 707.
62. Bynum, R. V., Hunter, W. E., Rogers, R. D. and Atwood, J. L., *Inorg. Chem.*, 1980, **19,** 2368.
63. Parker, K. G., Noll, B., Pierpont, C. G. and Rakowski Dubois, M., *Inorg. Chem.*, 1996, **35,** 3228.
64. Kabir, S. E., Rosenberg, E., Day, M., and Hardcastle, K. I., *Organometallics*, 1994, **13,** 4437.
65. Day, M., Espitia, D., Hardcastle, K. I., Kabir, S. E., McPhillips, T., Rosenberg, E., Gobetto, R., Milone, L. and Osella, D., *Organometallics*, 1993, **12,** 2309.
66. Day, M., Freeman, W., Hardcastle, K. I., Isomaki, M., Kabir, S. E., McPhillips, T., Rosenberg, E., Scott, L. G. and Wolf, E., *Organometallics*, 1992, **11,** 3376.
67. Day, M., Espitia, D., Hardcastle, K. I., Kabir, S. E., Rosenberg, E., Gobetto, R., Milone, L. and Osella, D., *Organometallics*, 1991, **10,** 3550.
68. Adams, R. D., Chen, L. and Wu, W., *Organometallics*, 1993, **12,** 4962.
69. Adams, R. D. and Chen, G., *Organometallics*, 1993, **12,** 2070.
70. Adams, R. D. and Tanner, J. T., *Appl. Organomet. Chem.*, 1992, **6,** 449.
71. Adams, R. D. and Chen, G., *Organometallics*, 1992, **11,** 3510.
72. Eisenstadt, A., Giandomenico, C. M., Fredericks, M. F. and Laine, R. M., *Organometallics*, 1985, **4,** 2033.
73. Giandomenico, C. M., Eisenstadt, A., Fredericks, M. F., Hirshon, A. S. and Laine, R. M., in *Catalysis of Organic Reactions*, ed. R. L. Augustine. Marcel Dekker, New York, 1985, p. 73.

74. Ledoux, M. J., Puges, P. E. and Maire, G., *J. Catal.*, 1982, **76,** 285.
75. Durfee, L. D., Fanwick, P. E., Rothwell, I. P., Folting, K. and Huffman, J. C., *J. Am. Chem. Soc.*, 1987, **109,** 4720.
76. Mayer, J. M., Curtis, C. J. and Bercaw, J. E., *J. Am. Chem. Soc.*, 1983, **105,** 2651.
77. Durfee, L. D., Hill, J. E., Kerschner, J. L., Fanwick, P. E. and Rothwell, I. P., *Inorg. Chem.*, 1989, **28,** 3095.
78. Chiu, K. W., Jones, R. A., Wilkinson, G., Galas, A. M. R. and Hursthouse, M. B., *J. Chem. Soc., Dalton Trans.*, 1981, 2088.
79. Adkins, H., Kuick, L. F., Farlow, M. and Wojcik, B., *J. Am. Chem. Soc.*, 1934, **56,** 2425.
80. Garnett, J. L. and Sollich, W. A., *J. Catal.*, 1963, **2,** 339.
81. Farragher, A. L. and Cossee, P., *Proc. 5th Int. Cong. Catal.*, ed. J. W. Hightower. North Holland, Amsterdam, 1973, p. 1301 ff.
82. Satterfield, C. N. and Cocchetto, J. F., *Ind. Engng. Chem. Process Des. Dev.*, 1981, **20,** 53.
83. Olalde, A. and Perot, G., *Appl. Catal.*, 1985, **13,** 373.
84. Satterfield, C. N., Modell, M., Hites, R. A. and Declerck, C. J., *Ind. Engng. Chem. Process Des. Dev.*, 1978, **17,** 141.
85. Vivier, L., Dominguez, V., Perot, G. and Kasztelan, S., *J. Molec. Catal.*, 1991, **67,** 267.
86. Shih, S. S., Katzer, J. R., Kwart, H. and Stiles, A. B., *Am. Chem. Soc., Div. Pet. Chem. Prepr.*, 1977, **22,** 919.
87. A highly loaded nickel oxide catalyst system that promotes C—N bond cleavage prior to hydrogenation of the arene ring in quinoline has been reported; see: Fish, R. H., Michaels, J. N., Moore, R. S. and Heinemann, H., *J. Catal.*, 1990, **123,** 74.
88. Miller, J. T. and Hinemann, M. F., *J. Catal.*, 1984, **85,** 117.
89. Laine, R. M., *New. J. Chem.*, 1987, **11,** 543.
90. Yang, S. H. and Satterfield, C. N., *J. Catal.*, 1983, **81,** 168.
91. Yang, S. H. and Satterfield, C. N., *Ind. Engng. Chem. Process Des. Dev.*, 1984, **23,** 20.
92. Satterfield, C. N., Smith, C. M. and Ingalls, M., *Ind. Engng. Chem. Process Des. Dev.*, 1985, **24,** 1000.
93. Satterfield, C. N. and Gültekin, S., *Ind. Engng. Chem. Process Des. Dev.*, 1981, **20,** 62.
94. Spies, G. H. and Angelici, R. J., *Organometallics*, 1987, **6,** 1897.
95. Ogilvy, A. E., Skaugset, A. E. and Rauchfuss, T. B., *Organometallics*, 1988, **7,** 1171.
96. Chen, J., Daniels, L. M. and Angelici, R. J., *J. Am. Chem. Soc.*, 1990, **112,** 199.
97. Chen, J., Daniels, L. M. and Angelici, R. J., *Polyhedron*, 1990, **9,** 1883.
98. Chen, J., Daniels, L. M. and Angelici, R. J., *J. Am. Chem. Soc.*, 1991, **113,** 2544.
99. Jones, W. D. and Dong, L., *J. Am. Chem. Soc.*, 1991, **113,** 559.
100. Dong, L., Duckett, S. B., Ohman, K. F. and Jones, W. D., *J. Am. Chem. Soc.*, 1992, **114,** 151.
101. Jones, W. D. and Chin, R. M., *Organometallics*, 1992, **11,** 2698.
102. Bianchini, C., Meli, A., Peruzzini, M., Vizza, F., Frediani, P., Herrera, V. and Sánchez-Delgado, R. A., *J. Am. Chem. Soc.*, 1993, **115,** 2731.
103. Laine, R. M., Thomas, D. W. and Cary, L. W., *J. Org. Chem.*, 1979, **44,** 4964.
104. Laine, R. M., Thomas, D. W. and Cary, L. W., *J. Am. Chem. Soc.*, 1982, **104,** 1763.
105. Kabir, S. E., Day, M., Irving, M., McPhillips, T., Minassian, H., Rosenberg, E. and Hardcastle, K. I., *Organometallics*, 1991, **10,** 3997.
106. Shvo, Y. and Laine, R. M., *J. Chem. Soc., Chem. Commun.*, 1980, 753.
107. Hiraki, K., Matsunaga, T. and Kawano, H., *Organometallics*, 1994, **13,** 1878.
108. Hagadorn, J. R. and Arnold, J., *Organometallics*, 1994, **13,** 4670.
109. Laine, R. M., *J. Mol. Catal.*, 1983, **21,** 119.
110. Hirschon, A. S. and Laine, R. M., *Fuel*, 1985, **64,** 911.
111. Hirschon, A. S. and Laine, R. M., *Fuel*, 1985, **64,** 868.
112. Satterfield, C. N. and Carter, D. L., *Ind. Engng. Chem. Proc. Des. Dev.*, 1981, **20,** 538.
113. Perot, G., *Catal. Today*, 1991, **10,** 447.
114. Fish, R. H., Thormodsen, A. D. and Heinemann, H., *J. Molec. Catal.*, 1985, **31,** 191.
115. Huckett, S. C., Miller, L. L., Jacobson, R. A. and Angelici, R. J., *Organometallics*, 1988, **7,** 686.
116. Angelici, R. J., *Acc. Chem. Res.*, 1988, **21,** 387.
117. Laine, R. M., Thomas, D. W., Cary, L. W. and Buttrill, S. E., *J. Am. Chem. Soc.*, 1978, **100,** 6527.
118. Lowry, T. H. and Richardson, K. S., *Mechanism and Theory in Organic Chemistry*, 3rd edn. Harper & Row, New York, 1987.
119. McLain, S. J., Sancho, J. and Schrock, R. R., *J. Am. Chem. Soc.*, 1980, **102,** 5610.
120. Wigley, D. E. and Gray, S. D., in *Comprehensive Organometallic Chemistry II*, Vol. 5, ed. E. W. Abel, F. G. A. Stone and G. Wilkinson. Pergamon Press. Oxford, 1995, pp. 57–153.
121. Bunel, E., Burger, B. J. and Bercaw, J. E., *J. Am. Chem. Soc.*, 1988, **110,** 976.
122. McNeill, K., Andersen, R. A. and Bergman, R. G., *J. Am. Chem. Soc.*, 1995, **117,** 3625.
123. Summers, M. F., Marzilli, L. G. and Box, A., *J. Am. Chem. Soc.*, 1986, **108,** 4285.
124. Bleeke, J. R., *Acc. Chem. Res.*, 1991, **24,** 271.
125. van der Heijden, H., Schaverien, C. J. and Orpen, A. G., *Organometallics*, 1989, **8,** 255.
126. Fish, R. H., Michaels, J. N., Moore, R. S. and Heinemann, H., *J. Catal.*, 1990, **123,** 75.
127. Weintreb, S. M. and Staib, R. R., *Tetrahedron*, 1982, **38,** 3087.
128. Fox, P. A., Bruck, M. A. and Wigley, D. E., unpublished results, 1996.
129. Yasuda, H., Kajihara, Y., Nagasuna, K., Mashima, K. and Nakamura, A., *Chem. Lett.*, 1981, 719.
130. Steffey, B. D., Chesnut, R. W., Kerschner, J. L., Pellechia, P. J., Fanwick, P. E. and Rothwell, I. P., *J. Am. Chem. Soc.*, 1989, **111,** 378.
131. Yasuda, H., Okamoto, T., Matsuoka, Y., Nakamura, A., Kai, Y., Kanehisa, N. and Kasai, N., *Organometallics*, 1989, **8,** 1139.
132. Eaton, B. E. and Rollman, B., *J. Am. Chem. Soc.*, 1992, **114,** 6245.

133. Kerr, C. E. and Eaton, B. E., *Organometallics*, 1995, **14,** 269.
134. Sigman, M. A., Kerr, C. E. and Eaton, B. E., *J. Am. Chem. Soc.*, 1993, **115,** 7545.
135. Erker, G., Engel, K., Krüger, C. and Chiang, A. P., *Chem. Ber.*, 1982, **115,** 3311.
136. Moreau, C., Bekakra, L., Durand, R. and Geneste, P., *Catal. Today*, 1991, **10,** 681.
137. Dzidic, I., Balicki, M. D., Petersen, H. A., Nowlin, J. G., Evans, W. E., Siegel, H. and Hart, H. V., *Energy Fuels*, 1991, **5,** 382.
138. Fish, R. H., in *Aspects of Homogeneous Catalysis*, ed. R. Ugo. Kluwer Academic Publishers, Amsterdam, 1990, pp. 65–83.
139. Rosales, M., Alvarado, Y., Boves, M., Rubio, R., Soscún, H. and Sánchez-Delgado, R. A., *Trans. Metal Chem.*, 1995, **20,** 246.
140. Maurya, R. C., Mishra, D. D., Pandey, M. and Awasthi, S., *Natl. Acad. Sci. Lett.*, 1990, **13,** 443.
141. Takahashi, Y., Onoyama, N. and Ishikawa, Y., *Chem. Lett.*, 1978, 525.
142. Bradley, D. C. and Thomas, I. M., *Proc. Chem. Soc.*, 1959, 225.
143. Bradley, D. C. and Thomas, I. M., *Can. J. Chem.*, 1961, **40,** 1355.
144. Bradley, D. C. and Gitlitz, M. H., *J. Chem. Soc. (A)*, 1969, 980.
145. Nugent, W. A., Ovenall, D. W. and Holmes, S. J., *Organometallics*, 1983, **2,** 161.
146. Berno, P. and Gambarotta, S., *Organometallics*, 1995, **14,** 2159.
147. Gambarotta, S., Abstracts of Papers, International Chemical Congress of Pacific Basin Societies, Honolulu, HI, 1995, American Chemical Society, Washington, DC, INOR 631, 1995.
148. Grasselli, R. K. and Burrington, J. D., *Adv. Catal.*, 1981, **30,** 133.
149. Burrington, J. D., Katisek, C. T. and Grasselli, R. K., *J. Catal.*, 1984, **81,** 489, and refs therein.
150. Maatta, E. A., Du, Y. and Rheingold, A. L., *J. Chem. Soc., Chem. Commun.*, 1990, 756.
151. Maatta, E. A. and Du, Y., *J. Am. Chem. Soc.*, 1988, **110,** 8249.
152. Chan, D. M.-T., Fultz, W. C., Nugent, W. A., Roe, D. C. and Tulip, T. H., *J. Am. Chem. Soc.*, 1985, **107,** 251.
153. Chan, D. M.-T. and Nugent, W. A., *Inorg. Chem.*, 1985, **24,** 1422.
154. Bakir, M., Fanwick, P. E. and Walton, R. A., *Inorg. Chem.*, 1988, **27,** 2016.
155. Rhodes, L. F. and Venanzi, L. M., *Inorg. Chem.*, 1987, **26,** 2692.
156. Han, S. H. and Geoffroy, G. L., *Polyhedron*, 1988, **7,** 2331.